DEPARTMENT OF THE NAVY

DAVID TAYLOR MODEL BASIN

HYDROMECHANICS

o

AERODYNAMICS

o

STRUCTURAL MECHANICS

o

APPLIED MATHEMATICS

ANALYSIS OF STRESSES AT JUNCTURES OF AXISYMMETRIC SHELLS WITH FLEXIBLE INSERT RINGS OF LINEARLY VARYING THICKNESS

by

Richard V. Raetz

STRUCTURAL MECHANICS LABORATORY
RESEARCH AND DEVELOPMENT REPORT

January 1961

Report 1444

DEPARTMENT OF THE NAVY
DAVID TAYLOR MODEL BASIN
WASHINGTON 7, D.C.

IN REPLY REFER TO
9110/Subs
5605
(705:MCC:
7-58
21 Feb 1961

From: Commanding Officer and Director, David Taylor Model Basin
To: Chief, Bureau of Ships (Code 335) (in duplicate)

Subj: S-F013 0302; Stresses at shell junctures reinforced by flexible insert rings; forwarding of report on

Encl: DATMOBAS Report 1444 entitled "Analysis of Stresses at Junctures of Axisymmetric Shells with Flexible Insert Rings of Linearly Varying Thickness" 3 copies

1. One of the possible methods of reducing the stresses at cone-cylinder junctures in submarine structures is to insert a tapered ring between the shells, its thickness at its edges being equal to that of the adjoining shells and gradually increasing toward its center. In enclosure (1) is presented a procedure for determining the stresses at such a juncture with or without additional reinforcement of the tapered ring.

2. Equations are derived for the elastic behavior of some typical shell junctures using insert rings with tapered sections. A numerical example is given which indicates that maximum discontinuity stresses in a typical reinforced cone-cylinder juncture would be reduced by 33 percent by the use of a flexible tapered ring.

E. E. Johnson

E.E. JOHNSON
By direction

Copy to:
BUSHIPS (106) with 1 copy of encl (1)
(321) with 1 copy of encl (1)
(420) with 1 copy of encl (1)
(421) with 1 copy of encl (1)
(423) with 1 copy of encl (1)
(440) with 1 copy of encl (1)
(442) with 2 copies of encl (1)

9110/Subs
5605
(705:MCC:lkg)
7-58
21 Feb 1961

Copy to:
BUSHIPS (443) with 1 copy of encl (1)
(525) with 1 copy of encl (1)
(633) with 1 copy of encl (1)
CHONR (439) with 2 copies of encl (1)
(466) with 1 copy of encl (1)
CNO (Op 702C) with 1 copy of encl (1)
CDR, USNOL, with 1 copy of encl (1)
DIR, USNRL, Attn: TID (Code 2027) with 1 copy of encl (1)
NAVSHIPYD PTSMH, with 2 copies of encl (1)
NAVSHIPYD MARE, with 2 copies of encl (1)
NAVSHIPYD NORVA, Attn: UERD (280) with 1 copy of encl (1)
SUPSHIP, Groton, with 1 copy of encl (1)
Electric Boat Div, General Dynamics Corp, with 1 copy of encl (1)
SUPSHIP, Newport News, with 1 copy of encl (1)
Newport News Shipbldg and Dry Dock Co, with 1 copy of encl (1)
SUPSHIP, Pascagoula, with 1 copy of encl (1)
Ingalls Shipbldg Corp, with 1 copy of encl (1)
DIR, DEF (R and E) Attn: Tech Library, with 1 copy of encl (1)
CO, USNROTC and NAVADMINU, MIT, with 1 copy of encl (1)
O in C, PGSCOL, Webb, with 1 copy of encl (1)
CDR, ASTIA, with 10 copies of encl (1)
OTS, Dept Comm, with 1 copy of encl (1)
Mr. H. Becker, with 1 copy of encl (1)

ANALYSIS OF STRESSES AT JUNCTURES OF AXISYMMETRIC SHELLS WITH FLEXIBLE INSERT RINGS OF LINEARLY VARYING THICKNESS

by

Richard V. Raetz

January 1961

Report 1444
S-F013 03 02

TABLE OF CONTENTS

LIST OF ILLUSTRATIONS

LIST OF TABLES

NOTATION

A	Cross-sectional area of ring
a, b, c, d, g, f	Coefficients representing edge rotation and displacement per unit edge or surface load
C_1, C_2, C_3, C_4	Arbitrary constants of integration
D	Flexural rigidity = $\dfrac{Eh^3}{12(1-\nu^2)}$
E	Young's modulus
H	Shearing force normal to axis of shell of revolution
$H_0^{(1)}, H_1^{(1)}$	Hankel Functions
h	Shell thickness
I	Moment of inertia about radial centroidal axis of ring
J_1, J_2	Bessel Functions
M	Moment in a meridional plane
N_x	Stress resultant in x-direction
N_ϕ	Stress resultant in ϕ-direction
P	Axial force
p	Pressure
Q	Shearing force normal to midplane surface of shell
R	Radius normal to axis
R_c	Radius of curvature = $R/\cos\alpha$
L, S_1, S_2	Dimensions associated with Figure 5
u	Displacement in the x-direction
w	Displacement normal to the midplane shell surface
$\overline{w}$	Displacement normal to the axis
X, Y, Z	Coordinates associated with Figure 5
x	Distance along the shell
y	Distance from apex of cone to origin of x-coordinate

NOTATION

α	Angle between axis of cone and generator of midplane surface
β	$\sqrt[4]{\frac{3\,(1-\nu^2)\cos^2\alpha}{R^2h^2}}$
γ	Constant of proportionality between thickness and distance x
δ_L, δ_R	Dimensions associated with Figure 7
ϵ	Strain
θ	Meridional rotation
ψ_1, ψ_2, ψ_3, ψ_4	Schleicher functions
ρ	$\sqrt[4]{\frac{12\,(1-\nu^2)\cos^2\alpha}{\gamma^2R^2}}$
σ	Stress
ν	Poisson's ratio
ξ	$2\rho\sqrt{x}$

ABSTRACT

The elastic deformations of a short, flexible, tapered ring under axisymmetric edge loading and uniform pressure are investigated. The ring is treated as a thin cylindrical or conical shell of short length and linearly varying thickness. A modified Geckeler-type approximation is used for the conical shell. Equations are derived for the elastic behavior of some typical shell junctures utilizing insert rings with tapered sections. A numerical example is given which indicates that maximum discontinuity stresses in a typical reinforced cone-cylinder juncture would be reduced by 33 percent by use of a flexible, tapered ring. The additional highly localized stresses due to notch effects have not been considered.

INTRODUCTION

A problem of concern to the designer of submarine pressure hulls is that of terminating axisymmetric cylindrical hull sections or of joining two such sections of different diameters with a reasonably short transition section. Truncated conical sections have become common, but high discontinuity stresses arise in the vicinities of the cylinder-cone junctures. These stresses result from the edge forces and moments exerted on the two shells by each other in enforcing structural continuity, since they do not tend to deform equally under pressure. Whereas high localized stresses may not immediately cause a failure of the hull, a fatigue failure may occur under cyclic loading. This is especially true of recent designs in which high-strength steels are used.

One of the possible methods of reducing discontinuity stresses is to insert a tapered ring between the shells, its thickness at its edges being equal to that of the adjoining shells and gradually increasing toward the center of its cross section; see Figure 1. A procedure for determining the stresses at such a juncture, with or without additional reinforcement of the ring, is described in this report.

In the following analysis, the ring is considered to be composed of short, linearly tapering sections of thin cylindrical or truncated conical shells. The first part of the problem is to find expressions for the deformations of such sections under pressure and edge loading and, from these, to derive edge coefficients. These edge coefficients are then used in the second part of the problem, which is to determine the edge forces and moments for all the components of the juncture.

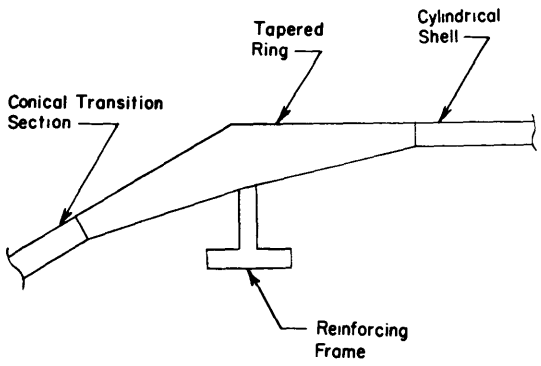

Figure 1 – Cross Section of Cone-Cylinder Juncture with Tapered Ring

Meissner[1] has derived expressions for the deflection of a tapered conical shell for the special case where the thickness becomes zero at the apex of the cone. Others[2] have applied a Geckeler-type approximation to the expressions for a cylindrical shell but have used additional simplifications which exclude geometries of interest here.

A Geckeler-type approximation, utilizing the well-known expressions for deflections of a cylindrical shell of varying thickness appearing in References 3 and 4, will be used here. A modification is then made when it is applied to very short shells.

For the second part of the problem, the procedure is much the same as that followed in Reference 5 in analyzing junctures with rigid insert rings. As in that report, the equations are applicable to any kind of shells for which edge coefficients can be found. A case of special interest to which this analysis is applicable is that of an "H" stiffener with a tapered faying flange on a conical shell.

A numerical example is given in which computed stresses at a typical cone-cylinder juncture containing a flexible, tapered, insert ring are compared with those at a juncture with a rigid insert ring.

DETERMINATION OF EDGE COEFFICIENTS FOR AN AXISYMMETRICAL CONICAL SHELL OF LINEARLY VARYING THICKNESS

The radial deflections and meridional rotations of the edges of the tapered shell are to be equated to those of the adjoining shells to enforce structural continuity. The assumptions and simplifications used in deriving the edge coefficients for these adjoining shells may, in general, be used in the following derivation to give approximately the same degree of accuracy. This degree of accuracy should be especially satisfactory if the highest stresses occur in the adjoining shells rather than in the tapered shell. It is expected that this will practically always be the case since the minimum thickness of the tapered shell should be at least equal to that of the adjoining shell.

Some of the simplifying assumptions used in the analysis are:

1. Thin shell theory may be applied.
2. Only elastic deformations occur.
3. Deflections are small so that they do not appreciably affect the point of application of the loads.
4. Shear deformations need not be accounted for.
5. The usual formulas relating the moments, curvatures, and cross-sectional moments of of inertia of uniform beams are applicable to beams of varying depth.

Additional assumptions will be discussed as they arise. Assumptions 1, 4, and 5 may be questioned since the tapered shell under consideration is relatively short and thick.

---

[1]References are listed on page 38.

Assumption 1 should still be easily justifiable because the only criterion to be satisfied is that the ratio of radius of curvature to maximum thickness be 10 or more.[3] Assumption 4 is made because the length-to-thickness ratio of the tapered shell, while much lower than that of the other shells, will still usually be two or more, based on the greatest thickness. A more conclusive reason for neglecting shear deformation, however, is that the maximum shear loads that may be applied to the edges of all the intersecting shells at the juncture will be of the same order of magnitude, and the shear deformations of the other shells, which will be equal to or greater than those of the tapered ring, may be neglected compared with their bending deformations. Thus shear deformations of the tapered shell would be important only for a very short shell subjected to very high shear loads, which cannot be applied by the long thin adjoining shells. Assumption 5 is discussed in Reference 6 where it is shown that the errors arising from this approximation would not exceed 4 percent even for a very high rate of taper, i.e., up to $\gamma = \frac{h}{x} \approx 0.83$; see Figure 2.

In this derivation the conical shell will be approximated by an "equivalent" cylindrical shell whose radius is equal to some representative radius of curvature of the conical shell. This is known as a Geckeler approximation and is widespread practice for shells of uniform thickness where the radius of the shell normal to the axis of symmetry does not change too rapidly along this axis.[5, 7] It has been shown[5, 7, 8] that this approximation is very satisfactory for cones of uniform thickness, the maximum error in computed deformations being about 5 percent when

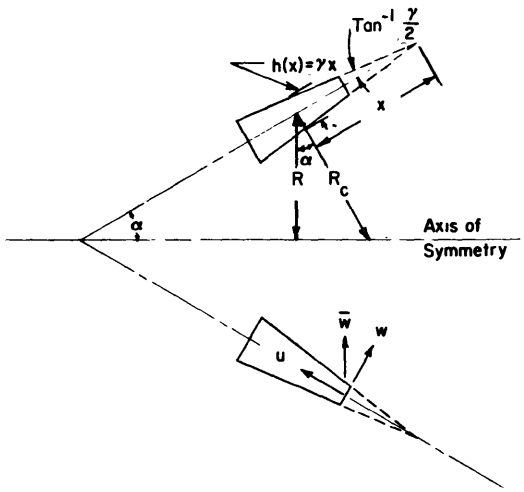

Figure 2 – Coordinate System for Conical Shell of Linearly Varying Thickness

$$\frac{2R\cos\alpha}{h\sin^2\alpha} = 60 \qquad [1]$$

For most cases of interest to the submarine designer this ratio will be much higher, with correspondingly lower errors due to this approximation.

BENDING ANALYSIS

The derivation of the differential equation of equilibrium of an axisymmetric cylindrical shell of linearly varying thickness is straightforward and is shown, together with the solution of the equation, in References 3 and 4. The homogeneous form of this equation is

$$\frac{d^2}{dx^2}\left(D\frac{d^2w_b}{dx^2}\right)+\frac{Eh}{R_c^2}w_b=0 \qquad [2]$$

where w_b is the bending component of w,

x is measured as shown in Figure 2,

$h = \gamma x$, and

$$D = \frac{Eh^3}{12(1-\nu^2)}$$

Furthermore, for the conical tapered shell, $R_c = R/\cos\alpha$. Equation [2] now becomes

$$\frac{d^2}{dx^2}\left(x^3\frac{d^2w_b}{dx^2}\right)+\frac{12(1-\nu^2)\cos^2\alpha}{\gamma^2 R^2}x\,w_b=0 \qquad [3]$$

It should be noted that Equation [3] and its solution are of the same type as the differential equations governing the axisymmetric deformations of a thin conical shell of constant thickness; see References 3 and 4.

The total deflection is

$$w = w_b + w_m \qquad [4]$$

where w_m is the membrane deflection.

From the solution of Equation [3] given in References 3 and 4, and from Equation [4],

$$w_b = \frac{1}{\sqrt{x}}[C_1\psi_1'(\xi) + C_2\psi_2'(\xi) + C_3\psi_3'(\xi) + C_4\psi_4'(\xi)]$$

$$w = \frac{1}{\sqrt{x}}[C_1\psi_1'(\xi) + C_2\psi_2'(\xi) + C_3\psi_3'(\xi) + C_4\psi_4'(\xi)] + w_m$$

$$\frac{dw}{dx} = \frac{1}{2x\sqrt{x}}\{C_1[\xi\psi_2(\xi) - 2\psi_1'(\xi)] - C_2[\xi\psi_1(\xi) + 2\psi_2'(\xi)]$$

$$+ C_3[\xi\psi_4(\xi) - 2\psi_3'(\xi)] - C_4[\xi\psi_3(\xi) + 2\psi_4'(\xi)]\} + \frac{dw_m}{dx}$$

$$M_x = D\frac{d^2w}{dx^2} = \frac{E\gamma^3}{48(1-\nu^2)}\sqrt{x}\,\{C_1[(\xi)^2\psi_2'(\xi) - 4\xi\psi_2(\xi) + 8\psi_1'(\xi)] \qquad [5]$$

$$- C_2[(\xi)^2\psi_1'(\xi) - 4\xi\psi_1(\xi) - 8\psi_2'(\xi)] + C_3[(\xi)^2\psi_4'(\xi) - 4\xi\psi_4(\xi) + 8\psi_3'(\xi)]$$

$$- C_4[(\xi)^2\,\psi_3'(\xi) - 4\,\xi\psi_3(\xi) - 8\,\psi_4'(\xi)]\} + D\,\frac{d^2 w_m}{dx^2}$$

$$Q_x = \frac{-dM_x}{dx} = \frac{E\gamma^3\,\rho^2}{24\,(1-\nu^2)}\,\sqrt{x}\{C_1[\xi\psi_1(\xi) + 2\psi_2'(\xi)] + C_2\,[\xi\psi_2(\xi) - 2\psi_1'(\xi)]$$

$$+ C_3[\xi\psi_3(\xi) + 2\psi_4'(\xi)] + C_4[\xi\psi_4(\xi) - 2\psi_3'(\xi)]\} - \frac{d}{dx}\left(D\,\frac{d^2 w_m}{dx^2}\right)$$

where C_1, C_2, C_3, and C_4 are arbitrary constants of integration,

$$\rho^4 = \frac{12(1-\nu^2)\cos^2\alpha}{\gamma^2\,R^2}, \text{ and}$$

$$\xi = 2\rho\sqrt{x}$$

The ψ functions appearing in Equations [5] are called Schleicher functions; they are defined as follows:

$$J_0\,(\sqrt{i}\,\xi) = \psi_1(\xi) + i\psi_2(\xi)$$

$$\sqrt{i}\,J_1\,(\sqrt{i}\,\xi) = \psi_1'(\xi) + i\psi_2'(\xi)$$

$$H_0^{(1)}(\sqrt{i}\,\xi) = \psi_3(\xi) + i\psi_4(\xi)$$

$$-\sqrt{i}\,H_1^{(1)}(\sqrt{i}\,\xi) = \psi_3'(\xi) + i\psi_4'(\xi)$$

where $i = \sqrt{-1}$,

J_0 and J_1 are Bessel functions of the first kind of orders zero and one, respectively,

$H_0^{(1)}$ and $H_1^{(1)}$ are Bessel functions of the third kind of orders zero and one, respectively,

and the primes denote differentitation with respect to ξ.

The assumption that the radius does not change rapidly in the area of the shell under consideration has been used in Equations [5], where the derivatives of ρ have been neglected. This is equivalent to the usual practice of neglecting the derivatives of the quantity

$$\beta = \sqrt[4]{\frac{3(1-\nu^2)\cos^2\alpha}{h^2\,R^2}} \qquad [6]$$

when applying the Geckeler approximation to shells of constant thickness.

Tables of numerical values of the ψ functions and their derivatives are given in References 3 and 4 for values of the argument ξ from zero to six, and in Reference 9 for values of ξ up to ten. For purposes of calculation, it might be necessary to use more significant figures for these ψ functions than are given in these tables. In such cases, the appropriate series expansions given in References 3 and 4 should be used. Where the tapered shell is used as an insert ring, it is expected that ξ will usually be less than six. For values of ξ greater than six the following convenient asymptotic formulas[3] may be used:

$$
\begin{aligned}
\psi_1(\xi) &= \frac{1}{\sqrt{2\pi\xi}}\, e^{\xi/\sqrt{2}} \cos\left(\frac{\xi}{\sqrt{2}} - \frac{\pi}{8}\right) \\
\psi_2(\xi) &= -\frac{1}{\sqrt{2\pi\xi}}\, e^{\xi/\sqrt{2}} \sin\left(\frac{\xi}{\sqrt{2}} - \frac{\pi}{8}\right) \\
\psi_1'(\xi) &= \frac{1}{\sqrt{2\pi\xi}}\, e^{\xi/\sqrt{2}} \cos\left(\frac{\xi}{\sqrt{2}} + \frac{\pi}{8}\right) \\
\psi_2'(\xi) &= -\frac{1}{\sqrt{2\pi\xi}}\, e^{\xi/\sqrt{2}} \sin\left(\frac{\xi}{\sqrt{2}} + \frac{\pi}{8}\right) \\
\psi_3(\xi) &= \sqrt{\frac{2}{\pi\xi}}\, e^{-\xi/\sqrt{2}} \sin\left(\frac{\xi}{\sqrt{2}} + \frac{\pi}{8}\right) \\
\psi_4(\xi) &= -\sqrt{\frac{2}{\pi\xi}}\, e^{-\xi/\sqrt{2}} \cos\left(\frac{\xi}{\sqrt{2}} + \frac{\pi}{8}\right) \\
\psi_3'(\xi) &= -\sqrt{\frac{2}{\pi\xi}}\, e^{-\xi/\sqrt{2}} \sin\left(\frac{\xi}{\sqrt{2}} - \frac{\pi}{8}\right) \\
\psi_4'(\xi) &= \sqrt{\frac{2}{\pi\xi}}\, e^{-\xi/\sqrt{2}} \cos\left(\frac{\xi}{\sqrt{2}} - \frac{\pi}{8}\right)
\end{aligned}
\qquad [7]
$$

Although Expressions [7] may not be applicable for the problems considered here, they do illustrate the general shape of the $\psi - \xi$ curves; see also Reference 4.

Thus far in the bending analysis it has not been necessary to specify whether the thin end of the shell was at the large or the small diameter edge of the truncated concial shell; that is, Equations [5] apply to both Cases A and B of Figure 3. However, in the determination of the membrane deflection w_m and its derivatives, the two cases of Figure 3 must be distinguished. In the following derivation, where double algebraic signs appear, the upper sign applies to Case A, and the lower sign applies to Case B.

The loading that will give rise to the membrane terms consists of uniform pressure and an axial force P, which includes the axial component of force resulting from the pressure; see Figure 4.

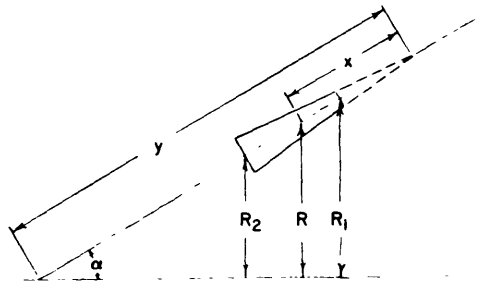

Figure 3a – Case A

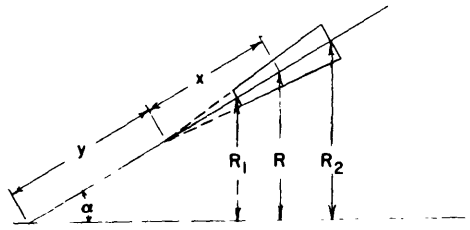

Figure 3b – Case B

Figure 3 – Two Types of Truncated Conical Shells of Linearly Varying Thickness

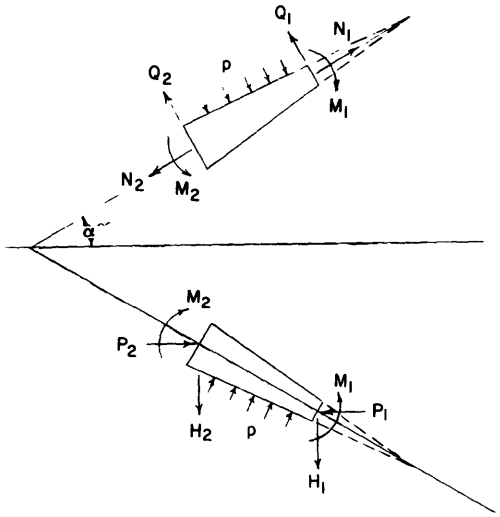

Figure 4 – Applied Loads

MEMBRANE ANALYSIS

From statics, it can be seen that

$$N_{x_m} = -\frac{P}{\cos\alpha}$$

$$N_{\phi_m} = -\frac{pR}{\cos\alpha} \qquad [8]$$

Also from geometry of deformation,

$$\bar{w}_m = -R\epsilon_{\phi_m} = w_m \cos\alpha \pm u_m \sin\alpha \quad [9]$$

Note here that the displacement u is taken positive in the direction of positive x. Rewriting [9] as

$$w_m = \frac{\bar{w}_m}{\cos\alpha} \mp u_m \tan\alpha \qquad [10]$$

and differentiating with respect to x gives

$$\frac{du_m}{dx} = \frac{1}{\cos\alpha}\frac{d\bar{w}_m}{dx} \mp \tan\alpha \frac{du_m}{dx} \qquad [11]$$

From the two-dimensional Hooke's law and Equations [9] and [8], it is seen that

$$\bar{w}_m = -\frac{R}{E\gamma x}(N_{\phi_m} - \nu N_{xm}) = \frac{pR^2 - \nu PR}{E\gamma x \cos\alpha} \qquad [12]$$

and

$$\frac{du_m}{dx} = \epsilon_{x_m} = \frac{1}{E\gamma x}(N_{x_m} - \nu N_{\phi_m}) = \frac{\nu pR - P}{E\gamma x \cos\alpha} \qquad [13]$$

It can be seen from Figure 3 that

$$R = (y \mp x) \sin \alpha$$

so that

$$\frac{dR}{dx} = \mp \sin \alpha \qquad [14]$$

Summing forces in the axial direction, we obtain

$$PR = \frac{pR^2}{2} + \left(P_1 R_1 - \frac{pR_1^2}{2} \right) = \frac{pR^2}{2} + \left(P_2 R_2 - \frac{pR_2^2}{2} \right) \qquad [15]$$

Now from Equations [12], [13], [14], and [15], Expression [11] for $\frac{dw_m}{dx}$ may be evaluated.

$$\frac{dw_m}{dx} = - \frac{pR^2 - \nu PR}{E\gamma x^2 \cos^2 \alpha} \mp \frac{(2pR - P) \sin \alpha}{E\gamma x \cos^2 \alpha} \qquad [16]$$

Also, from differentiation of Equation [16],

$$D \frac{d^2 w_m}{dx^2} = \frac{\gamma^2}{12 (1-\nu^2) \cos^2 \alpha} \left\{ 2(pR^2 - \nu PR) \pm x \sin \alpha \ [pR(4-\nu) - P] + x^2 \sin^2 \alpha \left(p + \frac{P}{R} \right) \right\} \qquad [17]$$

A second differentiation yields

$$\frac{d}{dx} \left(D \frac{d^2 w_m}{dx^2} \right) = \frac{\gamma^2}{12 (1-\nu^2) \cos^2 \alpha} \left\{ \mp \sin \alpha \ (P - \nu pR) - x \sin^2 \alpha \left[p (1-\nu) - \frac{P}{R} \right] \mp x^2 \sin^3 \alpha \left(\frac{p}{R} - \frac{2P}{R^2} \right) \right\} \qquad [18]$$

The last three expressions, Equations [16], [17], and [18], show that the order of magnitude of succeeding terms in each is reduced by the factor $\frac{x \sin \alpha}{R}$, so that usually the last term in each of Equations [17] and [18] may be neglected.

DETERMINATION OF INTEGRATION CONSTANTS FOR TAPERED SHELLS

The constants C_1, C_2, C_3, and C_4 in Equations [5] may now be evaluated from the boundary conditions. These conditions are:

$$
\begin{aligned}
(M_x)_1 &\equiv M_1 = D\frac{d^2w_1}{dx^2} \\
(Q_x)_1 &\equiv Q_1 = -\frac{d}{dx}\left(D\frac{d^2w_1}{dx^2}\right) \\
(M_x)_2 &\equiv M_2 = D\frac{d^2w_2}{dx^2} \\
(Q_x)_2 &\equiv Q_2 = \frac{d}{dx}\left(D\frac{d^2w_2}{dx^2}\right)
\end{aligned}
\qquad [19]
$$

where M_1, M_2, Q_1, and Q_2 are the applied edge moments and edge shears.

Note that the sign for the quantity Q_2 is positive since both edge shearing forces are defined as positive outward as shown in Figure 4. Substituting these boundary conditions in the last two of Equations [5], we obtain the following simultaneous algebraic equations to determine the constants C_1, C_2, C_3, and C_4:

$$
\begin{aligned}
\bar{M}_1 \equiv \frac{48(1-\nu^2)}{E\gamma^3\sqrt{x_1}}\left[M_1 - D_1\frac{d^2w_{m1}}{dx^2}\right] &= C_1\left[(\xi_1)^2\,\psi_2'(\xi_1) - 4\xi_1\psi_2(\xi_1) + 8\psi_1'(\xi_1)\right] \\
&\quad - C_2\left[(\xi_1)^2\,\psi_1'(\xi_1) - 4\xi_1\psi_1(\xi_1) - 8\psi_2'(\xi_1)\right] \\
&\quad + C_3\left[(\xi_1)^2\,\psi_4'(\xi_1) - 4\xi_1\psi_4(\xi_1) + 8\psi_3'(\xi_1)\right] \\
&\quad - C_4\left[(\xi_1)^2\,\psi_3'(\xi_1) - 4\xi_1\psi_3(\xi_1) - 8\psi_4'(\xi_1)\right] \\
\bar{M}_2 \equiv \frac{48(1-\nu^2)}{E\gamma^3\sqrt{x_2}}\left[M_2 - D_2\frac{d^2w_{m2}}{dx^2}\right] &= C_1\left[(\xi_2)^2\,\psi_2'(\xi_2) - 4\xi_2\psi_2(\xi_2) + 8\psi_1'(\xi_2)\right] \\
&\quad - C_2\left[(\xi_2)^2\,\psi_1'(\xi_2) - 4\xi_2\psi_1(\xi_2) - 8\psi_2'(\xi_2)\right]
\end{aligned}
\qquad [20]
$$

$$+ C_3 [(\xi_2)^2 \psi_4'(\xi_2) - 4\xi_2\psi_4(\xi_2) + 8\psi_3'(\xi_2)]$$

$$- C_4 [(\xi_2)^2 \psi_3'(\xi_2) - 4\xi_2\psi_3(\xi_2) - 8\psi_4'(\xi_2)]$$

$$\bar{Q}_1 \equiv \frac{24(1-\nu^2)}{E\gamma^3\rho^2\sqrt{x_1}}\left[Q_1 + \frac{d}{dx}\left(D_1 \frac{d^2 w_{m1}}{dx^2}\right)\right] = C_1[\xi_1\psi_1(\xi_1) + 2\psi_2'(\xi_1)] + C_2[\xi_1\psi_2(\xi_1) - 2\psi_1'(\xi_1)]$$

$$+ C_3[\xi_1\psi_3(\xi_1) + 2\psi_4'(\xi_1)] + C_4[\xi_1\psi_4(\xi_1) - 2\psi_3'(\xi_1)]$$

$$\bar{Q}_2 \equiv -\frac{24(1-\nu^2)}{E\gamma^3\rho^2\sqrt{x_2}}\left[Q_2 - \frac{d}{dx}\left(D_2 \frac{d^2 w_{m2}}{dx^2}\right)\right] = C_1[\xi_2\psi_1(\xi_2) + 2\psi_2'(\xi_2)] + C_2[\xi_2\psi_2(\xi_2) - 2\psi_1'(\xi_2)]$$

$$+ C_3[\xi_2\psi_3(\xi_2) + 2\psi_4'(\xi_2)] + C_4[\xi_2\psi_4(\xi_2) - 2\psi_3'(\xi_2)] \qquad [20]$$

Once the constants C_1, C_2, C_3, and C_4 are determined in terms of the applied edge moments and shears, M_1, M_2, Q_1, and Q_2, from Equations [20], then the deflection and slope at any point of the tapered shell element can be determined from Equations [5].

Long Tapered Shells

The functions ψ_1 and ψ_2 and their derivatives become increasingly larger with increasing ξ, while ψ_3 and ψ_4 become smaller. Since, for a long shell, the loading at one edge would not affect the deformations at the other, it is clear that for the thin edge (Edge 1), the constants C_1 and C_2 could be taken equal to zero and only the first and third equations in [20] used to determine C_3 and C_4. Since algebraic solution for C_3 and C_4 would be cumbersome whereas a numerical solution would be much simpler, the algebraic solution is not shown. Now C_3 and C_4, which are known in terms of M_1, Q_1, and p, may be substituted into Equations [5] along with Equations [12] and [16] and the relationships

$$\bar{w} = w_b \cos\alpha + \bar{w}_m \qquad [21]$$

and

$$Q_1 = H_1 \cos\alpha \pm P_1 \sin\alpha \qquad [22]$$

to obtain $\bar{w}_1$ and $\frac{dw_1}{dx}$ in terms of M_1, H_1, P_1, and p.

Similarly, to find the deformation at the thick edge (Edge 2), let C_3 and C_4 be equal to zero and find C_1 and C_2. Proceeding as before, but noting that

$$Q_2 = H_2 \cos \alpha \mp P_2 \sin \alpha, \qquad [23]$$

$\bar{w}_2$ and $\frac{du_2}{dx}$ may be found in terms of M_2, H_2, P_2, and p.

In general, the shell may be considered as "long" if each ψ function, when evaluated at one edge, is much larger or smaller than that evaluated at the other edge. This may be determined from an inspection of tables of functions. Where $\xi \geq 6$, a criterion could be derived from the asymptotic formulas, Equations [7]. It can be shown that the ψ functions change drastically within one-half wavelength of the trigonometric functions. In other words, the two edges are independent of each other when $\frac{\xi_2 - \xi_1}{\sqrt{2}} \geq \pi$. This is analogous to the requirement that the quantity βl be equal to or greater than π for a shell of uniform thickness.[5]

Note that, for a long conical shell where interaction between the two edges is neglected, the quantity ρ should be computed separately for each edge, using the radius at that edge.

Short Tapered Shells

For shells of short length where there is interaction between the two edges, Equations [20] should be solved simultaneously to obtain the four constants in terms of M_1, M_2, Q_1, Q_2, and p. Substituting these values together with Equations [12], [16], and [21] into Equation [5] then gives $\bar{w}$ and $\frac{dw}{dx}$.

At this point, it is apparent that, if the shell is very short and thick, has a large radius, and has an appreciable cone angle, as will be the case in many practical problems, an error arising from the use of the Geckeler approximation becomes large. This is true whether the thickness is constant or varying, but in either case may be readily corrected as will be shown.

The deformations of the shell may be considered to consist of two components: that of a rigid ring whose meridional cross section does not deform, and that due to bending of the meridional cross section. For a long shell, deformations due to edge loads are composed almost entirely of the second type, i.e., flexibility component, while, as the shell becomes shorter, it approaches the case of the rigid ring.

If deformations due to flexibility are denoted by the subscript f, the moment or force causing the deformation is denoted by a superscript, and the percentage difference in the radii of the edges of the shell is small enough that it may be regarded as a thin ring, then the expression for the total deflection of a flexible ring may be derived by inspection of Figure 5 to be

$$\bar{w}_1 = \left[w_{f1}^{M1} \cos\alpha + \frac{S_1 \cos\alpha\, R^2}{EI_{ZZ}} \right] M_1 + \left[w_{f1}^{M2} \cos\alpha - \frac{S_1 \cos\alpha\, R^2}{EI_{ZZ}} \right] M_2$$

$$+ \left[w_{f1}^{Q1} \cos\alpha - \frac{\cos\alpha\, R^2}{EA} - \frac{S_1^2 \cos\alpha\, R^2}{EI_{ZZ}} \right] Q_1$$

$$+ \left[w_{f1}^{Q2} \cos\alpha - \frac{\cos\alpha\, R^2}{EA} + \frac{S_1 S_2 \cos\alpha\, R^2}{EI_{ZZ}} \right] Q_2$$

$$+ \left[- \frac{\sin\alpha\, R^2}{EA} \right] N_1 + \left[\frac{\sin\alpha\, R^2}{EA} \right] N_2 + \frac{pL \cos\alpha\, R^2}{EA} + \frac{\left(S_1 - \frac{L}{2}\right) p \cos\alpha\, R^2}{EI_{ZZ}} \quad [24]$$

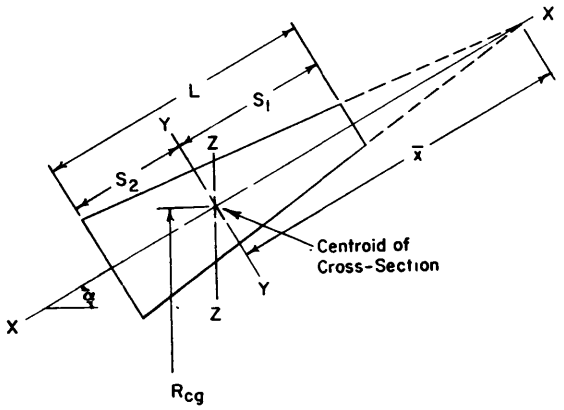

Figure 5 – Position of Centroid of Tapered Shell Section

Those terms in Equation [24] which have EA or EI in their denominator are the rigid-body deflections. Some small deformations due to Poisson's ratio are not included here but are included in the w_m terms in the shell solution.

With the following relationships, which can be obtained directly from Figure 4,

$$Q_1 = H_1 \cos\alpha + P_1 \sin\alpha$$

$$N_1 = H_1 \sin\alpha - P_1 \cos\alpha$$

$$Q_2 = H_2 \cos\alpha - P_2 \sin\alpha$$

$$N_2 = - H_2 \sin\alpha - P_2 \cos\alpha$$

Equation [24] then becomes:

$$\bar{w}_1 = \left[w_{f1}^{M1} \cos\alpha + \frac{S_1 \cos\alpha\, R^2}{EI_{ZZ}} \right] M_1 + \left[w_{f1}^{M2} \cos\alpha - \frac{S_1 \cos\alpha\, R^2}{EI_{ZZ}} \right] M_2$$

$$+\left[w_{f1}^{Q1}\cos^2\alpha - \frac{R^2}{EA} - \frac{S_1^2\cos^2\alpha\ R^2}{EI_{ZZ}}\right]H_1$$

$$+\left[w_{f1}^{Q2}\cos^2\alpha - \frac{R^2}{EA} + \frac{S_1S_2\cos^2\alpha\ R^2}{EI_{ZZ}}\right]H_2$$

$$+\left[w_{f1}^{Q1}\sin\alpha\cos\alpha - \frac{S_1^2\sin\alpha\cos\alpha\ R^2}{EI_{ZZ}}\right]P_1$$

$$+\left[-w_{f1}^{Q2}\sin\alpha\cos\alpha - \frac{S_1S_2\sin\alpha\cos\alpha\ R^2}{EI_{ZZ}}\right]P_2$$

$$+\frac{pL\cos\alpha\ R^2}{EA} + \frac{\left(S_1 - \frac{L}{2}\right)p\cos\alpha\ R^2}{EI_{ZZ}} \qquad [25]$$

An expression for $\bar{w}_1$ which is similar in form to Equation [24] and which can be found from the thin-shell analysis given earlier may be written, and this result may then be rewritten in terms similar to those of Equation [25]. Here, again, the coefficient of each edge moment and edge shear is made up of a flexibility component and a rigid-body component as in Equation [24]. The numerical solution for the bending components resulting from the thin-shell analysis, however, is for a cylinder with a radius of $R/\cos\alpha$. If this value of radius is taken to be that to the centroid of the shell cross section (Figure 5), the following expression for $\bar{w}_1$ may be deduced:

$$\bar{w}_1 = \left[w_{f1}^{M1}\cos\alpha + \frac{S_1\cos\alpha\ R^2}{EI_{YY}\cos^2\alpha}\right]\left(M_1 - D_1\frac{d^2w_{m1}}{dx^2}\right)$$

$$+\left[w_{f1}^{M2}\cos\alpha - \frac{S_1\cos\alpha\ R^2}{EI_{YY}\cos^2\alpha}\right]\left(M_2 - D_2\frac{d^2w_{m2}}{dx^2}\right)$$

$$+\left[w_{f1}^{Q1}\cos\alpha - \frac{\cos\alpha\ R^2}{EA\cos^2\alpha} - \frac{S_1^2\cos\alpha\ R^2}{EI_{YY}\cos^2\alpha}\right]\left(Q_1 + \frac{d}{dx}D_1\frac{d^2w_{m1}}{dx^2}\right)$$

$$+\left[w_{f1}^{Q2}\cos\alpha - \frac{\cos\alpha\ R^2}{EA\cos^2\alpha} + \frac{S_1S_2\cos\alpha\ R^2}{EI_{YY}\cos^2\alpha}\right]\left(Q_2 - \frac{d}{dx}D_2\frac{d^2w_{m2}}{dx^2}\right) + \bar{w}_{m1} \qquad [26]$$

For convenience in the comparison that follows, the contribution of the membrane deformations to the moment and shearing forces have been grouped with these corresponding terms in parentheses. If we let the quantities in parentheses in Equation [26] be denoted by M_1^*, M_2^*, Q_1^*, and Q_2^*, respectively, and note that,

$$Q_1^* = H_1^* \cos\alpha + P_1^* \sin\alpha$$

and

$$Q_2^* = H_2^* \cos\alpha - P_2^* \sin\alpha$$

where

$$H_1^* = H_1 + \frac{d}{dx} D_1 \frac{d^2 w_{m1}}{dx^2} \cos\alpha$$

$$P_1^* = P_1 + \frac{d}{dx} D_1 \frac{d^2 w_{m1}}{dx^2} \sin\alpha$$

$$H_2^* = H_2 - \frac{d}{dx} D_2 \frac{d^2 w_{m2}}{dx^2} \cos\alpha$$

$$P_2^* = P_2 + \frac{d}{dx} D_2 \frac{d^2 w_{m2}}{dx^2} \sin\alpha$$

then, the expression for $\bar{w}_1$ can be rewritten in the form

$$\bar{w}_1 = \left[w_{f1}^{M1} \cos\alpha + \frac{S_1 \cos\alpha R^2}{EI_{YY} \cos^2\alpha} \right] M_1^* + \left[w_{f1}^{M2} \cos\alpha - \frac{S_1 \cos\alpha R^2}{EI_{YY} \cos^2\alpha} \right] M_2^*$$

$$+ \left[w_{f1}^{Q1} \cos^2\alpha - \frac{\cos^2\alpha R^2}{EA \cos^2\alpha} - \frac{S_1^2 \cos^2\alpha R^2}{EI_{YY} \cos^2\alpha} \right] H_1^*$$

$$+ \left[w_{f1}^{Q2} \cos^2\alpha - \frac{\cos^2\alpha R^2}{EA \cos^2\alpha} + \frac{S_1 S_2 \cos^2\alpha R^2}{EI_{YY} \cos^2\alpha} \right] H_2^*$$

$$+ \left[w_{f1}^{Q1} \sin\alpha \cos\alpha - \frac{\sin\alpha \cos\alpha R^2}{EA \cos^2\alpha} - \frac{S_1^2 \sin\alpha \cos\alpha R^2}{EI_{YY} \cos^2\alpha} \right] P_1^*$$

$$+ \left[-w_{f1}^{Q2} \sin\alpha \cos\alpha + \frac{\sin\alpha \cos\alpha R^2}{EA \cos^2\alpha} - \frac{S_1 S_2 \sin\alpha \cos\alpha R^2}{EI_{YY} \cos^2\alpha} \right] P_2^* + \bar{w}_{m1} \qquad [27]$$

Now, the discrepancies between Equation [25], which was arrived at by consideration of Figure 5, and Equation [27], which was deduced from the thin-shell analysis, may be seen. First, the effect of the meridional force N on $\bar{u}_1$ is not shown in deducing Equation [27] as it was in finding Equation [25]. Note, however, that, with the aid of Figure 4, N_1 and N_2 can be expressed as

$$N_1 = -\frac{P_1}{\cos\alpha} + Q_1 \tan\alpha$$

$$N_2 = -\frac{P_2}{\cos\alpha} - Q_2 \tan\alpha \qquad [28]$$

In this form N is separated into a component due to a distributed load (the first terms, P being a distributed load) and a concentrated load (the second terms). Displacement due to stretching by this concentrated load may be neglected, just as it would be for a long shell. However, for a short shell the rigid-body displacement due to this second term must be considered. This is given by

$$\bar{w}_1 = -\frac{R^2 \sin\alpha}{EA}(Q_1 \tan\alpha)$$

or

$$\bar{w}_1 = -\frac{\sin^2\alpha}{EA} H_1 - \frac{R^2 \sin^2\alpha \tan\alpha}{EA} P_1 \qquad [29]$$

The other component of N_1, i.e., $\frac{P_1}{\cos\alpha}$, has been accounted for in the membrane terms and their derivatives. The coefficients of P_1 in $\bar{w}_{m1}$ in Equation [27] plus all the starred quantities then must contain a rigid-body-displacement component which has the value $\frac{1}{\cos\alpha}\bar{w}_1^{N_1}$, so that

$$\bar{w}_1^{P_1} = \frac{R^2 \sin\alpha}{EA \cos\alpha} P_1 \qquad [30]$$

This coefficient of P_1 just cancels out the second term, which is obviously extraneous, in the bracketed coefficient of P_1^* in Equation [27]. The corresponding term in the coefficient of P_2^* is canceled out in a like manner.

The effect of omitting the rigid-body-displacement component of $\bar{w}_1^{N_1}$ in Equation [29] will now be considered. It can be seen that, if these terms and the corresponding ones for H_2 and P_2 are added to Equation [27], and if the apparently extraneous $\cos^2\alpha$ appearing in

the denominator of all the $\frac{R^2}{EA}$ terms is removed, the net result is that Equation [27] is unchanged. Thus one apparent error arising from the use of the Geckeler approximation is compensated for by a small force component which was neglected.

One difference between Equations [25] and [27] still remains to be resolved. The last term in each of the bracketed coefficients of Equation [27] contains the term $I_{YY} \cos^2\alpha$ instead of I_{ZZ} in Equation [25]. Since it can be shown that

$$I_{ZZ} = I_{YY} \cos^2\alpha + I_{XX} \sin^2\alpha$$

tnen it can be shown that $I_{YY} \cos^2\alpha$ is a good approximation of I_{ZZ} for relatively long shells but not for the case of flexible insert rings (short shells) for which this analysis is to be applicable. The first terms within the brackets of Equation [27], which are predominant for long shells, may be considered correct, except for small errors introduced by the underlying assumptions discussed on page 2 of this report.

It is suggested that the last terms in the brackets of Equation [27] be computed and then extracted numerically from the total bracketed coefficients obtained directly from the analysis. Then each of these terms can be multiplied by the ratio

$$\frac{I_{YY} \cos^2\alpha}{I_{YY} \cos^2\alpha + I_{XX} \sin^2\alpha}$$

or

$$\frac{1}{1 + \frac{I_{XX}}{I_{YY}} \tan^2\alpha} \qquad [31]$$

and then returned to the bracketed coefficients.

It can be shown that similar corrections should be made to the expressions for $\bar{w}_2$, $\frac{dw_1}{dx}$, and $\frac{dw_2}{dx}$. In the case of $\frac{dw_1}{dx}$ and $\frac{dw_2}{dx}$, there is no problem concerning the effect of a concentrated edge load in the direction of N or of translation terms $\left(\frac{R^2}{EA} \text{ terms}\right)$, since they do not contribute to meridional rotation.

The terms thus derived to be added to the moment and force coefficients are given in Table 1. Each term is to be multiplied by

$$\left(\frac{R^2}{EI_{YY} \cos^2\alpha} - \frac{R^2}{EI_{ZZ}}\right) \qquad [32]$$

TABLE 1

Correction Terms for the Moment and Force Coefficients

	M_1^*	M_2^*	Q_1^*	Q_2^*
$\bar{w}_1$	$-S_1 \cos\alpha$	$+S_1 \cos\alpha$	$+S_1^2 \cos\alpha$	$-S_1 S_2 \cos\alpha$
$\bar{w}_2$	$+S_2 \cos\alpha$	$-S_2 \cos\alpha$	$-S_1 S_2 \cos\alpha$	$+S_2^2 \cos\alpha$
$\frac{dw_1}{dx}$	$+1$	-1	$-S_1$	$+S_2$
$\frac{dw_2}{dx}$	$+1$	-1	$-S_1$	$+S_2$

The derivation of expressions for I_{YY}, I_{XX}, A, and the x-coordinate of the centroid $\bar{x}$ for a tapered shell is straightforward; the expressions are

$$I_{YY} = \frac{\gamma}{4}(x_2^4 - x_1^4) - \frac{2\gamma}{9}\frac{(x_2^3 - x_1^3)^2}{x_2^2 - x_1^2}$$

$$I_{XX} = \frac{\gamma^3}{48}(x_2^4 - x_1^4) \qquad [33]$$

$$A = \frac{\gamma}{2}(x_2^2 - x_1^2)$$

$$\bar{x} = \frac{2(x_2^3 - x_1^3)}{3(x_2^2 - x_1^2)}$$

It should be noted that the correction procedure outlined above will not be important when the resultant moment on the component tapered rings is small and there is little meridional rotation of the insert ring as a whole. This will usually be the case in a well-designed ring.

The edge displacement and rotation thus found are functions of M_1, M_2, H_1, H_2, P_1, and P_2. P_1 and P_2 are usually considered known, however, since they may be computed directly from considerations of axial force equilibrium.

In this analysis as applied to short shells, although P_1 or P_2 may be arbitrary, $(P_1 - P_2)$ is specified as a function of pressure, and the effect of this quantity is included

in the coefficients of p. Therefore, the coefficients of P_1 and P_2 do not contain the complete effect of these two forces, although the total of the three coefficients of P_1, P_2, and p multiplied by their corresponding forces is correct. This means that the coefficients of P_1 and P_2 as derived for a short shell are suitable only when the distributed load, if any, is due to pressure and P_1 and P_2 are known.

DEFINITION OF EDGE COEFFICIENTS

The sign convention for the moments and shearing forces and for the deformations of the edges are chosen to facilitate the use of the edge coefficients in complicated juncture problems. The positive directions of the applied moments, forces, and pressure are shown in Figure 4. The deflections w and $\bar{w}$ are positive inward, and the positive direction of x is taken away from the edge. The coefficients of the moments, forces, and pressure in the expressions for $\bar{w}_1$, $\bar{w}_2$, and $\frac{dw_1}{dx}$ are the desired edge coefficients. The algebraic signs of all the terms in the expression for $\frac{dw_2}{dx}$, must be reversed, however, for the thick edge, because in their derivation, x was taken as positive toward the edge.

The nomenclature for the edge coefficients is chosen to be consistent with that used in Reference 5. The edge coefficients are defined as follows:

$$
\begin{aligned}
a_1^{(1)} &= \text{coefficient of } M_1 \text{ in } \frac{dw_1}{dx} \\
a_1^{(2)} &= \text{coefficient of } M_2 \text{ in } \frac{dw_1}{dx} \\
b_1^{(1)} &= \text{coefficient of } H_1 \text{ in } \frac{dw_1}{dx} \\
b_1^{(2)} &= \text{coefficient of } H_2 \text{ in } \frac{dw_1}{dx} \\
c_1 &= [\text{coefficient of } P_1] \frac{P_1}{p} + [\text{coefficient of } P_2] \frac{P_2}{p} \\
&\quad + [\text{coefficient of } p] \text{ in } \frac{dw_1}{dx} \\
d_1^{(1)} &= \text{coefficient of } M_1 \text{ in } \bar{w}_1 \\
d_1^{(2)} &= \text{coefficient of } M_2 \text{ in } \bar{w}_1 \\
g_1^{(1)} &= \text{coefficient of } H_1 \text{ in } \bar{w}_1 \\
g_1^{(2)} &= \text{coefficient of } H_2 \text{ in } \bar{w}_1
\end{aligned}
\qquad [34]
$$

$$f_1 = [\text{coefficient of } P_1]\,\frac{P_1}{p} + [\text{coefficient of } P_2]\,\frac{P_2}{p} + [\text{coefficient of } p] \text{ in } \bar{w}_1 \qquad [34]$$

Here the subscript for edge coefficients denotes the edge at which the deformation occurs, and the superscript denotes the edge at which the corresponding load is applied. For Edge 2, the subscript 2 is used for the edge coefficients, $\frac{dw}{dx}$ and $\bar{w}$ are evaluated at Edge 2, and the sign of $\frac{dw}{dx}$ is reversed.

The total edge rotations and edge displacements are then given by superposition to be

$$\begin{aligned}
\theta_1 &\equiv \frac{dw_1}{dx} = a_1^{(1)} M_1 + a_1^{(2)} M_2 + b_1^{(1)} H_1 + b_1^{(2)} H_2 + c_1 p \\
\theta_2 &\equiv -\frac{dw_2}{dx} = a_2^{(1)} M_1 + a_2^{(2)} M_2 + b_2^{(1)} H_1 + b_2^{(2)} H_2 + c_2 p \\
\bar{w}_1 &= d_1^{(1)} M_1 + d_1^{(2)} M_2 + g_1^{(1)} H_1 + g_1^{(2)} H_2 + f_1 p \\
\bar{w}_2 &= d_2^{(1)} M_1 + d_2^{(2)} M_2 + g_2^{(1)} H_1 + g_2^{(2)} H_2 + f_2 p
\end{aligned} \qquad [35]$$

DETERMINATION OF MOMENTS AND SHEARING FORCES

Moments and shearing forces at the juncture shown in Figure 1 will now be analyzed. All the components of the juncture are first separated, and the necessary moments and forces are placed at the boundaries. These moments and forces and their nomenclature are shown in Figure 6.

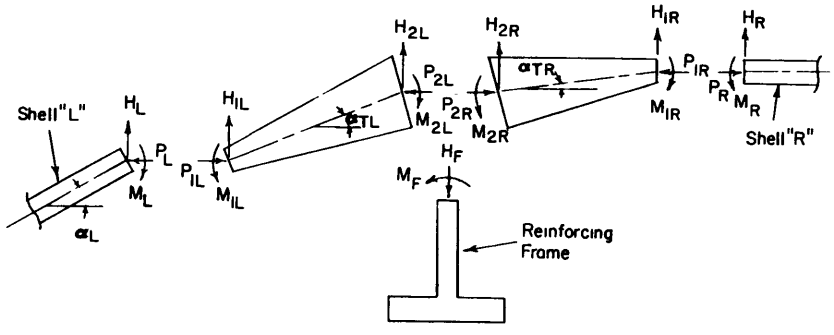

Figure 6 – Nomenclature and Sign Convention for Moments and Forces in Juncture of Figure 1

Force and moment equilibrium at the three junctures shown in Figure 6 require:

$$\begin{aligned} M_L &= M_{1L} \\ H_L &= -H_{1L} \\ P_L &= P_{1L} \\ M_R &= M_{1R} \\ H_R &= -H_{1R} \\ P_R &= P_{1R} \\ M_{2R} - M_{2L} &= M_F \\ H_{2L} + H_{2R} &= H_F \\ P_{2L} &= P_{2R} \end{aligned} \qquad [36]$$

Continuity of displacements and rotations at these three junctures require:

$$\begin{aligned} \bar{w}_L &= \bar{w}_{1L} \\ \theta_L &= -\theta_{1L} \\ \bar{w}_R &= \bar{w}_{1R} \\ \theta_R &= -\theta_{1R} \\ \bar{w}_{2L} &= \bar{w}_{2R} = \bar{w}_F \\ \theta_{2L} &= -\theta_{2R} = \theta_F \end{aligned} \qquad [37]$$

The deformations of the reinforcing frame may be expressed as

$$\begin{aligned} \bar{w}_F &= k_a H_F \\ \theta_F &= k_b M_F \end{aligned} \qquad [38]$$

If the frame is not too deep, the thin-ring formulas may be used for the stiffnesses k_a and k_b. Thus

$$\begin{aligned} k_a &= \frac{R_{2L}}{R_F} \frac{R_F^2}{EA_F} = \frac{R_{2L} R_F}{EA_F} \\ k_b &= \frac{R_{2L} R_F}{EI_F} \end{aligned} \qquad [39]$$

where A_F is the cross-sectional area of the frame,

I_F is the moment of inertia about the radial centroidal axis of the frame, and

R_F is the radius to the centroid of the frame.

In Equations [39] the differences between the radius of the point of application of M_F and H_F and the radii R_{2L} and R_{2R} are neglected.

The remaining quantities appearing in the continuity conditions [37] may be expressed in terms of edge coefficients and the corresponding moments, forces, and pressure. It is assumed that the adjoining shells labeled "L" and "R" in Figure 6 are of semi-infinite length. Thus

$$
\begin{aligned}
\bar{w}_L &= d_L M_L + g_L H_L + f_L p \\
\theta_L &= a_L M_L + b_L H_L + c_L p \\
\bar{w}_R &= d_R M_R + g_R H_R + f_R p \\
\theta_R &= a_R M_R + b_R H_R + c_R p \\
\bar{w}_{1L} &= d_{1L}^{(1L)} M_{1L} + d_{1L}^{(2L)} M_{2L} + g_{1L}^{(1L)} H_{1L} + g_{1L}^{(2L)} H_{2L} + f_{1L} p \\
\theta_{1L} &= a_{1L}^{(1L)} M_{1L} + a_{1L}^{(2L)} M_{2L} + b_{1L}^{(1L)} H_{1L} + b_{1L}^{(2L)} H_{2L} + c_{1L} p \\
\bar{w}_{1R} &= d_{1R}^{(1R)} M_{1R} + d_{1R}^{(2R)} M_{2R} + g_{1R}^{(1R)} H_{1R} + g_{1R}^{(2R)} H_{2R} + f_{1R} p \\
\theta_{1R} &= a_{1R}^{(1R)} M_{1R} + a_{1R}^{(2R)} M_{2R} + b_{1R}^{(1R)} H_{1R} + b_{1R}^{(2R)} H_{2R} + c_{1R} p \\
\bar{w}_{2L} &= d_{2L}^{(1L)} M_{1L} + d_{2L}^{(2L)} M_{2L} + g_{2L}^{(1L)} H_{1L} + g_{2L}^{(2L)} H_{2L} + f_{2L} p \\
\theta_{2L} &= a_{2L}^{(1L)} M_{1L} + a_{2L}^{(2L)} M_{2L} + b_{2L}^{(1L)} H_{1L} + b_{2L}^{(2L)} H_{2L} + c_{2L} p \\
\bar{w}_{2R} &= d_{2R}^{(1R)} M_{1R} + d_{2R}^{(2R)} M_{2R} + g_{2R}^{(1R)} H_{1R} + g_{2R}^{(2R)} H_{2R} + f_{2R} p \\
\theta_{2R} &= a_{2R}^{(1R)} M_{1R} + a_{2R}^{(2R)} M_{2R} + b_{2R}^{(1R)} H_{1R} + b_{2R}^{(2R)} H_{2R} + c_{2R} p
\end{aligned}
\qquad [40]
$$

The definition and nomenclature of the edge coefficients is given by Equations [34].

Now, if Equations [40], [38], and [36] are substituted into Equation [37], the following equations are obtained:

$$
\begin{aligned}
&(a_L + a_{1L}^{(1L)})M_L + (b_L - b_{1L}^{(1L)})H_L + a_{1L}^{(2L)} M_{2L} + b_{1L}^{(2L)} H_{2L} = -(c_L + c_{1L})p \\
&(a_R + a_{1R}^{(1R)})M_R + (b_R - b_{1R}^{(1R)})H_R + a_{1R}^{(2R)} M_{2R} + b_{1R}^{(2R)} H_{2R} = -(c_R + c_{1R})p \\
&(d_L - d_{1L}^{(1L)})M_L + (g_L + g_{1L}^{(1L)})H_L - d_{1L}^{(2L)} M_{2L} - g_{1L}^{(2L)} H_{2L} = (f_{1L} - f_L)p \\
&(d_R - d_{1R}^{(1R)})M_R + (g_R + g_{1R}^{(1R)})H_R - d_{1R}^{(2R)} M_{2R} - g_{1R}^{(2R)} H_{2R} = (f_{1R} - f_R)p \\
&a_{2L}^{(1L)} M_L - b_{2L}^{(1L)} H_L + (a_{2L}^{(2L)} + k_b) M_{2L} - k_b M_{2R} + b_{2L}^{(2L)} H_{2L} = -c_{2L} p \\
&a_{2R}^{(1R)} M_R - b_{2R}^{(1R)} H_R - k_b M_{2L} + (a_{2R}^{(2R)} + k_b) M_{2R} + b_{2R}^{(2R)} H_{2R} = -c_{2R} p \\
&d_{2L}^{(1L)} M_L - g_{2L}^{(1L)} H_L + d_{2L}^{(2L)} M_{2L} + (g_{2L}^{(2L)} - k_a) H_{2L} - k_a H_{2R} = -f_{2L} p \\
&d_{2R}^{(1R)} M_R - g_{2R}^{(1R)} H_R + d_{2R}^{(2R)} M_{2R} - k_a H_{2L} + (g_{2R}^{(2R)} - k_a) H_{2R} = -f_{2R} p
\end{aligned}
\qquad [41]
$$

These eight equations may be solved numerically for the moments and shear forces appearing in them, and the remaining unknown moments and forces may then be found from Equations [36].

Another case of interest is that in which the reinforcing frame of Figure 6 is removed. Then M_F and H_F in Equations [36] are zero. The eight equations then derived are identical to Equations [41] with k_a and k_b set equal to zero.

One other case, shown in Figure 7, will be covered since it represents a type of juncture commonly used in the design of submarine pressure hulls. In this case Shells L, R, and 3 are taken to be of semi-infinite length. The insert ring and reinforcing frame are considered to act as a unit. Therefore, if it is desired to analyze a similar juncture without the frame, it is simply deleted when the cross-sectional properties of the ring are computed. The pressures on Shells L and 3 are assigned subscripts L and 3, respectively, to preserve their identities, since the two shells obviously cannot both be loaded with the same pressure simultaneously. Ordinarily either p_L or p_3 is equal to p, and the other is equal to zero. Furthermore, the axial forces P_L and P_3 are not, in general, equal to $pR/2$, although they are usually linear functions of pressure. Determination of these two forces requires consideration of the remaining pressure hull structure not shown in Figure 7 and, where one of the forces is not zero, may involve some method of apportionment of the total axial force between the two shells. It is assumed that these forces may be determined with satisfactory accuracy without consideration of the deformations of the juncture.

The resultant moment M_F and force H_F on the rigid ring-and-frame combination may be determined by static equilibrium to be

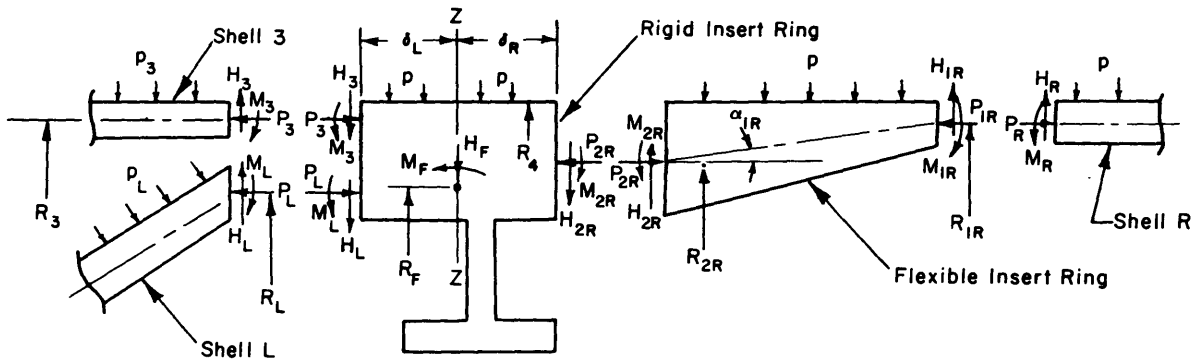

Figure 7 – Nomenclature and Sign Convention for Moments and Forces in Three-Shell Juncture

$$M_F = \frac{R_L}{R_F} M_L + \delta_L \frac{R_L}{R_F} H_L + \frac{R_3}{R_F} M_3 + \delta_L \frac{R_3}{R_F} H_3 - \frac{R_{2R}}{R_F} M_{2R} - \delta_R \frac{R_{2R}}{R_F} H_{2R}$$

$$- (R_L - R_F) P_L - (R_3 - R_F) P_3 + (R_{2R} - R_F) P_{2R} + \frac{(\delta_L^2 - \delta_R^2)}{2} \frac{R_4}{R_F} p \qquad [42]$$

$$H_F = \frac{R_L}{R_F} H_L + \frac{R_3}{R_F} H_3 + \frac{R_{2R}}{R_F} H_{2R} + (\delta_L + \delta_R) \frac{R_4}{R_F} p$$

It can also be seen that the continuity conditions are given by

$$\begin{aligned}
\theta_L &= \theta_3 = -\theta_{2R} = \theta_F \\
\bar{w}_L &= \bar{w}_3 = \bar{w}_F + \delta_L \theta_F \\
\bar{w}_{2R} &= \bar{w}_F - \delta_R \theta_F \\
\theta_{1R} &= -\theta_R \qquad [43] \\
\bar{w}_{1R} &= \bar{w}_R \\
M_{1R} &= M_R \\
H_{1R} &= -H_R
\end{aligned}$$

If it is assumed that the composite ring and frame deforms as a thin ring of rigid cross section, then these deformations are given by

$$\theta_F = k_b M_F$$
$$\bar{w}_F = k_a H_F \qquad [44]$$

where A_F is the cross-sectional area of ring and frame,

I_F is the moment of inertia of ring-and-frame combination about a radial centroidal axis,

$k_a = \dfrac{R_F^2}{EA_F}$, and

$k_b = \dfrac{R_F^2}{EI_F}$.

The deformations of all the shell edges may be expressed in terms of edge coefficients as was done in Equations [40] with the following exceptions. For Shells L and 3 the coefficients c and f, which include deformations due to both radial pressure and axial force P (which is assumed to be $pR/2$), must be replaced with separate coefficients for each of these two loads. Thus

$$\begin{aligned}
\theta_L &= a_L M_L + b_L H_L + c_L' P_L + c_L'' p_L \\
\bar{w}_L &= d_L M_L + g_L H_L + f_L' P_L + f_L'' p_L \\
\theta_3 &= a_3 M_3 + b_3 H_3 + c_3' P_3 + c_3'' p_3 \\
\bar{w}_3 &= d_3 M_3 + g_3 H_3 + f_3' P_3 + f_3'' p_3
\end{aligned} \qquad [45]$$

Equations [42] through [45], together with the required expressions from Equations [40], may be combined to give the following ten equations which may be solved for the unknown moments and shearing forces.

$$\begin{aligned}
a_L M_L + b_L H_L - k_b M_F &= - c_L' P_L - c_L'' p_L \\
d_L M_L + g_L H_L - \delta_L k_b M_F - k_a H_F &= - f_L' P_L - f_L'' p_L \\
a_3 M_3 + b_3 H_3 - k_b M_F &= - c_3' P_3 - c_3'' p_3 \\
d_3 M_3 + g_3 H_3 - \delta_L k_b M_F - k_a H_F &= - f_3' P_3 - f_3'' p_3
\end{aligned} \qquad [46]$$

$$-(a_R + a_{1R}^{(1R)}) M_{1R} - a_{1R}^{(2R)} M_{2R} + (b_R - b_{1R}^{(1R)}) H_{1R} - b_{1R}^{(2R)} H_{2R} = (c_R + c_{1R}) p$$

$$(d_R - d_{1R}^{(1R)}) M_{1R} - d_{1R}^{(2R)} M_{2R} - (g_R + g_{1R}^{(1R)}) H_{1R} - g_{1R}^{(2R)} H_{2R} = (f_{1R} - f_R) p$$

$$a_{2R}^{(1R)} M_{1R} + a_{2R}^{(2R)} M_{2R} + b_{2R}^{(1R)} H_{1R} + b_{2R}^{(2R)} H_{2R} + k_b M_F = - c_{2R} p$$

$$d_{2R}^{(1R)} M_{1R} + d_{2R}^{(2R)} M_{2R} + g_{2R}^{(1R)} H_{1R} + g_{2R}^{(2R)} H_{2R} + \delta_R k_b M_F - k_a H_F = - f_{2R} p$$

$$R_L M_L + R_3 M_3 - R_{2R} M_{2R} - R_F M_F + \delta_L R_L H_L + \delta_L R_3 H_3 - \delta_R R_{2R} H_{2R} \qquad [46]$$

$$= R_F (R_L - R_F) P_L + R_F (R_3 - R_F) P_3 - R_F (R_{2R} - R_F) P_{2R} - \frac{R_4}{2} (\delta_L^2 - \delta_R^2) p$$

$$R_L H_L + R_3 H_3 + R_{2R} H_{2R} - R_F H_F = - (\delta_L + \delta_R) R_4 p$$

NUMERICAL EXAMPLE

The maximum stresses in the juncture shown in Figure 8 will be computed as a numerical example of the analysis described in this report. For convenience, the tapered shell element adjacent to the conical shell is designated "*TL*," and that adjacent to the cylindrical shell is designated "*TR*."

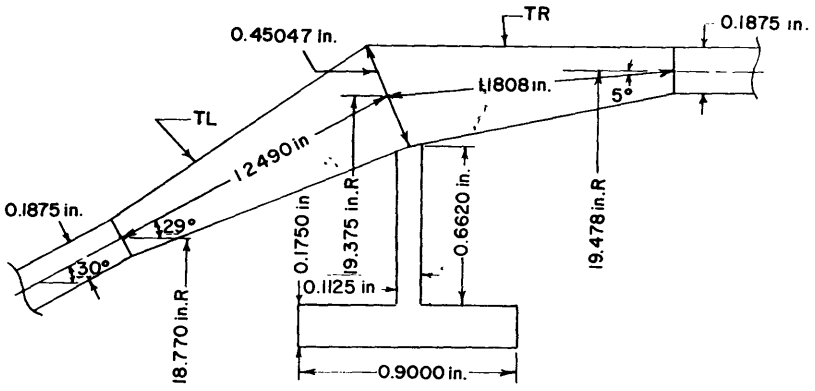

Figure 8 – Dimensions of Juncture Used in Numerical Example

The juncture elements are first separated as shown in Figure 6, and appropriate edge moments and forces are introduced using the same notation shown thereon. In the section on determination of edge coefficients (page 18), the subscripts 1 and 2 correspond to 1*L* and 2*L* and to 1*R* and 2*R*, respectively, for this particular application.

The dimensions shown in Figure 8 and quantities computed from Equations [33] are as follows. For tapered element *TL*:

$$\sin \alpha_{TL} = 0.4848$$

$$\cos \alpha_{TL} = 0.8746$$

$$\gamma_{TL} = 0.210543$$
$$x_{1L} = 0.89056 \text{ in.}$$
$$x_{2L} = 2.13956 \text{ in.}$$
$$\bar{x}_{TL} = 1.60087 \text{ in.}$$
$$L_{TL} = 1.249 \text{ in.}$$
$$S_{1L} = 0.71031 \text{ in.}$$
$$S_{2L} = 0.53869 \text{ in.}$$
$$R_{1L} = 18.770 \text{ in.}$$
$$R_{2L} = 19.375 \text{ in.}$$
$$R_{cg} = 19.114 \text{ in.}$$
$$A_{TL} = 0.402785 \text{ in.}^2$$
$$I_{YY} = 0.0488613 \text{ in.}^4$$
$$I_{XX} = 0.0039522 \text{ in.}^4$$
$$I_{ZZ} = 0.0383041 \text{ in.}^4$$
$$I_{YY} \cos^2 x = 0.0373752 \text{ in.}^4$$
$$I_{XX} \sin^2 x = 0.0009289 \text{ in.}^4$$
$$\rho_{TL} = 0.847734 \text{ in.}^{-\frac{1}{2}}$$
$$\xi_{1L} = 1.6$$
$$\xi_{2L} = 2.48$$

Shell TL is represented by Case B in Figure 3; wherever double signs are encountered, the lower sign will be used.

For tapered element TR:

$$\sin \alpha_{TR} = 0.0872$$
$$\cos \alpha_{TR} = 0.9962$$
$$\gamma_{TR} = 0.222703$$
$$x_{1R} = 0.841928 \text{ in.}$$
$$x_{2R} = 2.02273 \text{ in.}$$
$$\bar{x}_{TR} = 1.51345 \text{ in.}$$
$$L_{TR} = 1.1808 \text{ in.}$$
$$S_{1R} = 0.67152 \text{ in.}$$
$$S_{2R} = 0.50928 \text{ in.}$$

$$R_{1R} = 19.478 \text{ in.}$$
$$R_{2R} = 19.375 \text{ in.}$$
$$R_{cg} = 19.422 \text{ in.}$$
$$A_{TR} = 0.376657 \text{ in.}^2$$
$$I_{YY} = 0.0412858 \text{ in.}^4$$
$$I_{XX} = 0.00373685 \text{ in.}^4$$
$$I_{ZZ} = 0.0410004 \text{ in.}^4$$
$$I_{YY} \cos^2\alpha = 0.0409720 \text{ in.}^4$$
$$I_{XX} \sin^2\alpha = 0.0000284 \text{ in.}^4$$
$$\rho_{TR} = 0.871846 \text{ in.}^{-\frac{1}{2}}$$
$$\xi_{1R} = 1.6$$
$$\xi_{2R} = 2.48$$

Shell TR is represented by Case A in Figure 3 so the upper signs will be used when double signs occur.

Note that the dimensions of the tapered elements have been arbitrarily selected to simplify the computations so that

$$\xi_{1L} = \xi_{1R}$$
$$\xi_{2L} = \xi_{2R}$$

It is assumed that the juncture is part of a closed pressure vessel and that, at any point,

$$P = \frac{pR}{2}$$

Furthermore, in all subsequent computations, p will be taken to be +1 psi. Thus

$$P_{1L} = 9.3850$$
$$P_{2L} = 9.6875$$
$$P_{1R} = 9.7390$$
$$P_{2R} = 9.6875$$

From Reference 9, for $\xi_{1L} = \xi_{1R} = 1.6$,

$$\psi_1 = 0.8979 \qquad \psi_1' = -0.2545$$
$$\psi_2 = -0.6327 \qquad \psi_2' = -0.7727$$

$$\psi_3 = 0.1926 \qquad \psi_3' = -0.1788$$
$$\psi_4 = -0.0166 \qquad \psi_4' = 0.1560$$

and, for $\xi_{2L} = \xi_{2R} = 2.48$,

$$\psi_1 = 0.4186 \qquad \psi_1' = -0.9221$$
$$\psi_2 = -1.4372 \qquad \psi_2' = -0.9981$$
$$\psi_3 = 0.07238 \qquad \psi_3' = -0.09644$$
$$\psi_4 = 0.04413 \qquad \psi_4' = 0.01230$$

Note that most of the ψ functions differ from one edge to the other by a factor of only about 2. Furthermore

$$\frac{\xi_2 - \xi_1}{\sqrt{2}} = 0.622 < \pi$$

so that the tapered elements must be treated as "short shells" and all four constants of integration in Equations [5] must be retained. Derivation of edge coefficients for tapered element TL will be shown in detail. First, Equations [20] may be set up as follows.

$$\begin{aligned} M_{1L} &= 0.03517\,C_1 + 0.21648\,C_2 - 0.9248\,C_3 + 2.93837\,C_4 \\ \bar{M}_{2L} &= 0.74151\,C_1 + 1.83899\,C_2 - 1.13364\,C_3 + 1.40956\,C_4 \\ Q_{1L} &= -0.10876\,C_1 - 0.50332\,C_2 + 0.62016\,C_3 + 0.33104\,C_4 \\ Q_{2L} &= -0.95807\,C_1 - 1.72006\,C_2 + 0.20410\,C_3 + 0.30232\,C_4 \end{aligned} \qquad [47]$$

These equations may then be solved simultaneously for the constants C_1, C_2, C_3, and C_4, i.e.,

$$\begin{aligned} C_1 &= 5.15828\,\bar{M}_{1L} - 8.15432\,\bar{M}_{2L} - 5.04397\,\bar{Q}_{1L} - 6.59295\,\bar{Q}_{2L} \\ C_2 &= -3.05979\,\bar{M}_{1L} + 4.89541\,\bar{M}_{2L} + 3.29915\,\bar{Q}_{1L} + 3.30202\,\bar{Q}_{2L} \\ C_3 &= -1.58196\,\bar{M}_{1L} + 2.29749\,\bar{M}_{2L} + 2.99914\,\bar{Q}_{1L} + 1.37964\,\bar{Q}_{2L} \\ C_4 &= 0.006127\,\bar{M}_{1L} + 0.460016\,\bar{M}_{2L} + 0.761228\,\bar{Q}_{1L} + 0.269345\,\bar{Q}_{2L} \end{aligned}$$

Substituting these expressions along with the values of the ψ functions into Equations [5], we obtain

$$
\begin{aligned}
w_{b_{1L}}\sqrt{x_{1L}} &= 1.3354\,\bar{M}_{1L} - 2.0464\,\bar{M}_{2L} \\
&\quad -1.6831\,\bar{Q}_{1L} - 1.0782\,\bar{Q}_{2L} \\
w_{b_{2L}}\sqrt{x_{2L}} &= -1.5497\,\bar{M}_{1L} + 2.4171\,\bar{M}_{2L} \\
&\quad +1.0783\,\bar{Q}_{1L} + 2.6539\,\bar{Q}_{2L}
\end{aligned}
\qquad [48]
$$

$$
\begin{aligned}
\frac{dw_{b_{1L}}}{dx}\,(2x_{1L}\sqrt{x_{1L}}) &= -3.4566\,\bar{M}_{1L} + 5.1119\,\bar{M}_{2L} \\
&\quad +3.4182\,\bar{Q}_{1L} + 3.9668\,\bar{Q}_{2L} \\
\frac{dw_{b_{2L}}}{dx}\,(2x_{2L}\sqrt{x_{2L}}) &= -12.2837\,\bar{M}_{1L} + 19.3167\,\bar{M}_{2L} \\
&\quad +12.5880\,\bar{Q}_{1L} + 14.8659\,\bar{Q}_{2L}
\end{aligned}
$$

From the definitions given in Equations [20] and [26], for tapered element TL,

$$
\begin{aligned}
E\,\bar{M}_{1L} &= 4959.43\,M_{1L}^{*} \\
E\,\bar{M}_{2L} &= 3199.63\,M_{2L}^{*} \\
E\,\bar{Q}_{1L} &= 3450.52\,Q_{1L}^{*} \\
E\,\bar{Q}_{2L} &= -2226.13\,Q_{2L}^{*}
\end{aligned}
$$

Then, using these values and the relationship $\bar{w}_b = w_b \cos\alpha$, the following may be obtained from Equations [48]:

$$
\begin{aligned}
E\,\bar{w}_{b_{1L}} &= 6137.93\,M_{1L}^{*} - 6068.32\,M_{2L}^{*} - 5382.35\,Q_{1L}^{*} + 2224.48\,Q_{2L}^{*} \\
E\,\bar{w}_{b_{2L}} &= -4595.44\,M_{1L}^{*} + 4624.26\,M_{2L}^{*} + 2224.70\,Q_{1L}^{*} - 3532.51\,Q_{2L}^{*} \\
E\,\frac{dw_{b_{1L}}}{dx} &= -10199.1\,M_{1L}^{*} + 9731.06\,M_{2L}^{*} + 7017.15\,Q_{1L}^{*} - 5253.76\,Q_{2L}^{*} \\
E\,\frac{dw_{b_{2L}}}{dx} &= -9732.93\,M_{1L}^{*} + 9874.48\,M_{2L}^{*} + 6939.43\,Q_{1L}^{*} - 5287.20\,Q_{2L}^{*}
\end{aligned}
\qquad [49]
$$

The correction terms to be added to the moment and force coefficients appearing in Equations [49], using the results of Table 1, are

	M_{1L}^*	M_{2L}^*	Q_{1L}^*	Q_{2L}^*
$E\ \bar{w}_{b_{1L}}$	−147.25	+147.25	+104.59	− 79.32
$E\ \bar{w}_{b_{2L}}$	+111.67	−111.67	− 79.32	+ 60.15
$E\ \frac{dw_{b_{1L}}}{dx}$	+237.02	−237.02	−168.36	+127.68
$E\ \frac{dw_{b_{2L}}}{dx}$	+237.02	−237.02	−168.36	+127.68

so that Equations [49] become

$$
\begin{aligned}
E\ \bar{w}_{b_{1L}} &= 5990.68\ M_{1L}^* - 5921.07\ M_{2L}^* - 5277.76\ Q_{1L}^* + 2145.16\ Q_{2L}^* \\
E\ \bar{w}_{b_{2L}} &= -4483.77\ M_{1L}^* + 4512.59\ M_{2L}^* + 2145.38\ Q_{1L}^* - 3472.36\ Q_{2L}^* \\
E\ \frac{dw_{b_{1L}}}{dx} &= -9962.1\ M_{1L}^* + 9494.04\ M_{2L}^* + 6848.79\ Q_{1L}^* - 5126.08\ Q_{2L}^* \\
E\ \frac{dw_{b_{2L}}}{dx} &= -9495.91\ M_{1L}^* + 9637.46\ M_{2L}^* + 6771.07\ Q_{1L}^* - 5159.52\ Q_{2L}^*
\end{aligned}
\qquad [50]
$$

Now, from Equations [12], [16], [17], and [18] the membrane deformations for element TL are computed to be

$$
\begin{aligned}
E\ \bar{w}_{m_{1L}} &= 1826.05; & E\ \bar{w}_{m_{2L}} &= 809.914 \\
E\ \frac{dw_{m_{1L}}}{dx} &= -\ 2114.43; & E\ \frac{dw_{m_{2L}}}{dx} &= -\ 391.928 \\
D_{1L}\ \frac{d^2w_{m_{1L}}}{dx^2} &= 3.04065; & D_{2L}\ \frac{d^2w_{m_{2L}}}{dx^2} &= 3.04546 \\
\frac{d}{dx}\left(D_{1L}\ \frac{d^2w_{m_{1L}}}{dx^2}\right) &= 0.009437; & \frac{d}{dx}\left(D_{2L}\ \frac{d^2w_{m_{2L}}}{dx^2}\right) &= 0.009432
\end{aligned}
\qquad [51]
$$

The starred quantities appearing in Equations [50] may now be evaluated, and the membrane deformations may be added to give the total deformations. From the definitions associated with Equations [26], it is found that

$$M_{1L}^{*} = M_{1L} - 3.04065$$

$$M_{2L}^{*} = M_{2L} - 3.04546$$

$$Q_{1L}^{*} = Q_{1L} + 0.009437$$

$$Q_{2L}^{*} = Q_{2L} - 0.009432$$

Substituting these values of the starred quantities into Equation [50], we obtain

$$\begin{aligned} E\,\bar{w}_{1L} = E\,\bar{w}_{b_{1L}} + E\,\bar{w}_{m_{1L}} &= 5990.68\,M_{1L} - 5921.07\,M_{2L} \\ &\quad - 5277.76\,Q_{1L} + 2145.16\,Q_{2L} + 1826.05 \\ &\quad + (-18{,}215.6 + 18{,}032.4 - 49.8 - 20.2) \end{aligned} \qquad [52]$$

With the substitutions in Equations [22] and [23] and the numerical values of P_{1L} and P_{2L} Equation [52] becomes

$$E\,\bar{w}_{1L} = 5990.68\,M_{1L} - 5921.07\,M_{2L} - 4615.93\,H_{1L} + 1876.16\,H_{2L} + 35{,}660.6$$

Similarly,

$$E\,\bar{w}_{2L} = -4483.77\,M_{1L} + 4512.59\,M_{2L} + 1876.35\,H_{1L} - 3036.93\,H_{2L} - 25{,}315.5$$

$$E\,\frac{dw_{1L}}{dx} = -9962.1\,M_{1L} + 9494.04\,M_{2L} + 5989.95\,H_{1L} - 4483.27\,H_{2L} - 55{,}859 \qquad [53]$$

$$E\,\frac{dw_{2L}}{dx} = -9495.91\,M_{1L} + 9637.46\,M_{2L} + 5921.98\,H_{1L} - 4512.52\,H_{2L} - 55{,}795$$

Since every term in the eight simultaneous Equations [41] contains Young's modulus E as a factor, it has been removed from all terms to simplify the computations.

The edge coefficients defined by Equations [34] and [35] may now be written down for the tapered element TL by inspection of Equations [53]. Note that the signs of all terms in $E\,\frac{dw_{2L}}{dx}$ are reversed because of the sign convention adopted for θ_{2L}. Thus

$$Ea_{1L}^{(1L)} = -\ 9{,}962.1 \qquad Ed_{1L}^{(1L)} = \ 5{,}990.68$$

$$Ea_{1L}^{(2L)} = \ 9{,}494.04 \qquad Ed_{1L}^{(2L)} = -\ 5{,}921.07$$

$$Eb_{1L}^{(1L)} = \ 5{,}989.95 \qquad Eg_{1L}^{(1L)} = -\ 4.615.93$$

$$Eb_{1L}^{(2L)} = -\ 4{,}483.27 \qquad Eg_{1L}^{(2L)} = \ 1{,}876.16$$

$$Ec_{1L} = -55{,}859 \qquad Ef_{1L} = 35{,}660.6$$

$$Ea_{2L}^{(1L)} = 9{,}495.91 \qquad Ed_{2L}^{(1L)} = -4{,}483.77$$

$$Ea_{2L}^{(2L)} = -9{,}637.46 \qquad Ed_{2L}^{(2L)} = 4{,}512.59$$

$$Eb_{2L}^{(1L)} = -5{,}921.98 \qquad Eg_{2L}^{(1L)} = 1{,}876.35$$

$$Eb_{2L}^{(2L)} = 4{,}512.52 \qquad Eg_{2L}^{(2L)} = -3{,}036.93$$

$$Ec_{2L} = 55{,}795.0 \qquad Ef_{2L} = -25{,}315.5$$

The edge coefficients for the tapered element TR are derived in a similar manner. Note that in this example the equations for tapered element TR corresponding to Equations [47] and [48] can be obtained by replacing subscripts $1L$ and $2L$ with $1R$ and $2R$, respectively, wherever they appear in those equations. The correction terms in Table 1 are not used for this element because the difference between $I_{YY}\cos^2\alpha$ and I_{ZZ} is negligible. These coefficients are:

$$Ea_{1R}^{(1R)} = -9642.14 \qquad Ed_{1R}^{(1R)} = 6248.67$$

$$Ea_{1R}^{(2R)} = 9199.74 \qquad Ed_{1R}^{(2R)} = -6177.81$$

$$Eb_{1R}^{(1R)} = 6247.90 \qquad Eg_{1R}^{(1R)} = -5160.58$$

$$Eb_{1R}^{(2R)} = -4677.84 \qquad Eg_{1R}^{(2R)} = 2132.82$$

$$Ec_{1R} = 8550.8 \qquad Ef_{1R} = -4702.04$$

$$Ea_{2R}^{(1R)} = 9201.52 \qquad Ed_{2R}^{(1R)} = -4678.34$$

$$Ea_{2R}^{(2R)} = -9335.36 \qquad Ed_{2R}^{(2R)} = 4707.69$$

$$Eb_{2R}^{(1R)} = -6178.73 \qquad Eg_{2R}^{(1R)} = 2133.02$$

$$Eb_{2R}^{(2R)} = 4707.63 \qquad Eg_{2R}^{(2R)} = -3386.96$$

$$Ec_{2R} = -8518.0 \qquad Ef_{2R} = 5321.80$$

The edge coefficients for Shells L and R (Figure 6) are found from formulas given in Reference 5. These formulas apply to either conical or cylindrical shells. Where double signs appear, the upper and lower signs denote the large or small diameter end of a truncated cone, respectively.

Thus, for Shell L,

$$R_L = 18.770$$

$$h_L = 0.1875$$

$$\alpha_L = 30°$$

and

$$Ea_L = -\left[\sqrt[4]{12(1-\nu^2)}\right]^3 \sqrt{\frac{2R}{h^5 \cos \alpha}} = -2{,}598.01$$

$$Eb_L = \frac{\sqrt{12(1-\nu^2)}\, R}{h^2} = 1{,}764.25$$

$$Ec_L = \pm \frac{\sqrt{12\,(1-\nu^2)}\, R^2 \tan \alpha}{2h^2} \mp \frac{3R \tan \alpha}{2h \cos \alpha} = 9{,}459.08$$

[54]

$$Ed_L = \frac{\sqrt{12(1-\nu^2)}\, R}{h^2} = 1{,}764.25$$

$$Eg_L = -\sqrt[4]{12(1-\nu^2)} \sqrt{\frac{2R^3 \cos \alpha}{h^3}} = -2{,}396.14$$

$$Ef_L = \mp \sqrt[4]{12(1-\nu^2)} \sqrt{\frac{R^5 \sin^2 \alpha}{2h^3 \cos \alpha}} + \frac{\left(1 - \frac{\nu}{2}\right) R^2}{h \cos \alpha} = -11{,}138.9$$

For Shell R,

$$R_R = 19.478$$

$$h_R = 0.1875$$

$$\alpha_R = 0$$

and

$$Ea_R = -2462.93$$

$$Eb_R = 1830.87$$

$$E\,c_R = 0$$

$$E\,d_R = 1830.87$$

$$E\,g_R = -2722.03$$

$$E\,f_R = 1719.91$$

The cross-sectional properties of the frame are easily found to be

$$A_F = 0.231975 \text{ in.}^2$$

$$I_F = 0.0107098 \text{ in.}^4$$

From Equations [39] the frame stiffnesses are found to be

$$E\, k_a = 1{,}548.03$$

$$E\, k_b = 33{,}530.4$$

The eight simultaneous Equations [41] for finding the edge moments and forces then can be set up for numerical computation to be

$$\begin{aligned}
-12{,}560.1\, M_L - 4225.70\, H_L + 9494.04\, M_{2L} - 4483.27\, H_{2L} &= 46{,}400.0 \\
-12{,}105.1\, M_R - 4417.03\, H_R + 9199.74\, M_{2R} - 4677.84\, H_{2R} &= -8{,}550.8 \\
-4{,}226.43\, M_L - 7012.07\, H_L + 5921.07\, M_{2L} - 1876.16\, H_{2L} &= 46{,}799.5 \\
-4{,}417.80\, M_R - 7882.61\, H_R + 6177.81\, M_{2R} - 2132.82\, H_{2R} &= -6{,}421.95 \\
9495.91\, M_L + 5921.98\, H_L + 23{,}892.9\, M_{2L} - 33{,}530.4\, M_{2L} + 4512.52\, H_{2L} &= -55{,}795 \\
9201.52\, M_R + 6178.73\, H_R - 33{,}530.4\, M_{2L} + 24{,}195.0\, M_{2R} + 4707.63\, H_{2R} &= 8{,}518.0 \\
-4483.77\, M_L - 1876.35\, H_L + 4{,}512.59\, M_{2L} - 4{,}584.96\, H_{2L} - 1548.03\, H_{2R} &= 25{,}315.5 \\
-4678.34\, M_R - 2133.02\, H_R + 4{,}707.69\, M_{2R} - 1{,}548.03\, H_{2L} - 4934.99\, H_{2R} &= -5{,}321.80
\end{aligned} \qquad [55]$$

Solution of these eight simultaneous equations, together with Equations [36], leads to the following numerical values:

$$\begin{aligned}
M_L &= 0.472605 & M_{1L} &= 0.472605 \\
H_L &= -4.32543 & H_{1L} &= 4.32543 \\
M_R &= 0.809583 & M_{1R} &= 0.809583 \\
H_R &= 1.31510 & H_{1R} &= -1.31510 \\
M_{2L} &= 2.16329 & M_{2R} &= 2.16959 \\
H_{2L} &= -3.01554 & H_{2R} &= 2.75808 \\
M_F &= 0.0063 & H_F &= -0.25746
\end{aligned}$$

As an overall check on the calculations succeeding the determination of the edge coefficients, these edge moments and shears may be substituted into Equations [40], and the resulting deflections and slopes may be checked against the continuity conditions defined by Equations [37]. Such a check shows that

$$E\,\theta_L = 600 \qquad E\,\theta_{1L} = -601$$

$$E\,\bar{w}_L = 59.2 \qquad E\,\bar{w}_{1L} = 59.3$$

$$E\,\theta_R = 414 \qquad E\,\theta_{1R} = -414$$

$$E\,\bar{w}_R = -377.6 \qquad E\,\bar{w}_{1R} = -377.3$$

$$E\,\theta_{2L} = 211 \qquad E\,\theta_{2R} = -213$$

$$E\,\bar{w}_{2L} = -398.6 \qquad E\,\bar{w}_{2R} = -398.5$$

$$E\,\theta_F = 211$$

$$E\,\bar{w}_F = -398.6$$

Stresses and strains at any point in the tapered elements may now be computed from the following formulas:

Circumferential strain $$\epsilon_\phi = -\frac{\bar{w}}{R}$$

Longitudinal stress
$$\begin{cases} \sigma_x^0 = \dfrac{N}{h} + \dfrac{6M_x}{h^2} \approx -\dfrac{P}{h\cos\alpha} + \dfrac{6M_x}{h^2} \\ \sigma_x^i \approx -\dfrac{P}{h\cos\alpha} - \dfrac{6M_x}{h^2} \end{cases} \qquad [56]$$

Circumferential stress $$\sigma_\phi = E\,\epsilon_\phi + \nu\sigma_x$$

Longitudinal strain $$\epsilon_x = \frac{1-\nu^2}{E}\,\sigma_x - \nu\,\epsilon_\phi$$

where the superscripts "0" and "i" denote the external and internal surfaces, respectively.

To compute the stress and strain distributions for this problem a sufficient number of values of ξ are chosen between the edge values, 1.6 and 2.48, that may be found in tables of functions without involving interpolation. The values chosen are 1.8, 2.0, and 2.2. The values of x and R for each value of ξ are then found for each shell, and M_x may be computed from Equations [5] and [17]. Displacement $\bar{w}$ may be computed from Equations [5], [17], and [21].

The quantities of most interest are usually ϵ_ϕ, which is a measure of the radial deflection, and σ_x, which is the higher stress. Usually the maximum value of σ_x occurs at the shell edges and may be computed directly from the edge moments and Equations [56]. Distributions of ϵ_ϕ and σ_x for the tapered elements and for the adjoining conical and cylindrical shells in the vicinities of the junctures for this problem are given in Figure 9. The stress and strain curves for the constant-thickness conical and cylindrical shells were computed by methods described in Reference 5.

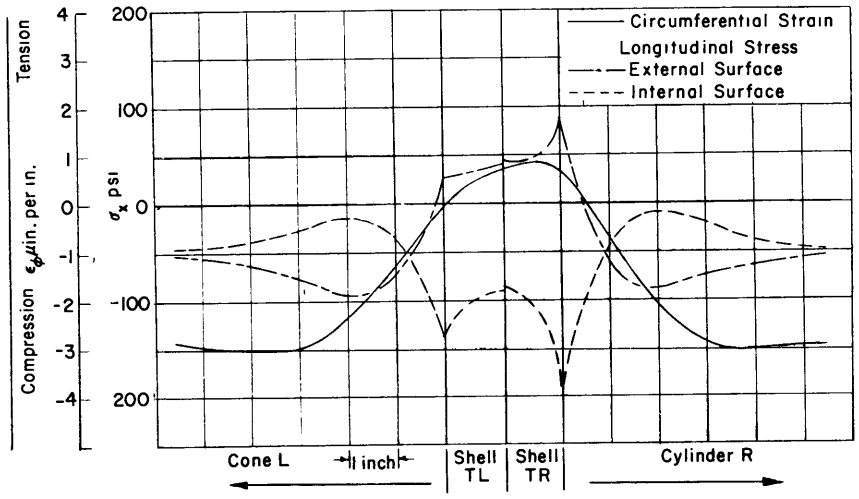

Figure 9 – Stresses and Strains in the Tapered Shell Juncture Example

The effect of the flexibility of the tapered juncture ring may be determined by analyzing[5] a similar juncture which includes a rigid insert ring with the same cross-sectional area as the combined tapered ring and frame and by comparing the computed strains and stresses. If it is assumed further that the near-optimum design for the rigid ring is used in which there is no meridional rotation, the edge moments and forces may be computed using the following boundary conditions

$$\theta_L = \theta_R = 0$$

$$\bar{w}_L = \bar{w}_R = \frac{R_T^2}{EA_T}(H_L + H_R) \qquad [57]$$

The geometric properties for the rigid insert are

$$A_T = A_F + A_{TL} + A_{TR} = 1.0114 \text{ in.}^2$$

$$R_T \approx 19.0 \text{ in.}$$

so that

$$\frac{R_T^2}{EA_T} = 356.924$$

The boundary conditions [57] may be combined with expressions for θ and $\bar{w}$ for the two shells, giving the following four simultaneous equations to be solved for the edge moments and forces:

$$\begin{aligned} a_L M_L + b_L H_L + c_L p &= 0 \\ d_L M_L + g_L H_L + f_L p &= k a_T (H_L + H_R) \\ a_R M_R + b_R H_R + c_R p &= 0 \\ d_R M_R + g_R H_R + f_R p &= k a_R (H_L + H_R) \end{aligned} \qquad [58]$$

Solving Equations [58] leads to

$$\begin{aligned} M_L &= 1.31463 \\ H_L &= -3.42562 \\ M_R &= 1.27330 \\ H_R &= 1.71287 \end{aligned}$$

Curves of ϵ_ϕ and σ_x distributions for the rigid insert are given in Figure 10. Since the ring in this case is assumed to be rigid and does not bend, longitudinal strains in the ring cross section would be negligible and hence are not shown thereon.

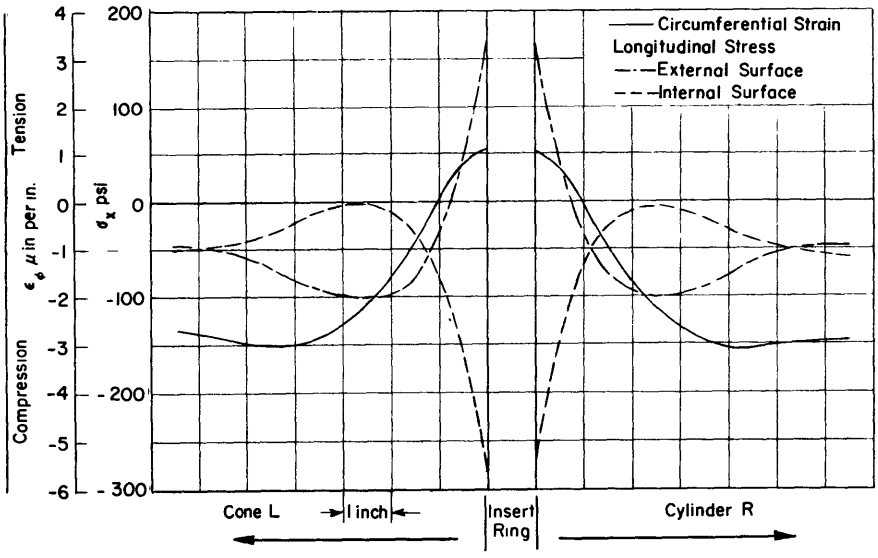

Figure 10 – Stresses and Strains in the Rigid Ring Juncture Example

In the tapered-ring analysis it was found that the maximum longitudinal stress sensitivity occurs at the edge of the cylinder and is −190 psi/psi as compared with a longitudinal membrane stress sensitivity of −52 psi/psi. From the rigid-ring analysis, the maximum longitudinal stress sensitivity occurs at the edge of the cone and is −282 psi/psi as compared with a longitudinal membrane stress sensitivity of −58 psi/psi.

SUMMARY AND CONCLUSIONS

The entire procedure described in this report for analyzing the stresses at a juncture in a composite shell structure such as that shown in Figure 1 is illustrated with the numerical example. The results of this computation are compared with those for a similar juncture with a rigid insert ring of approximately the same cross-sectional area as the tapered ring. The computations indicate that the maximum longitudinal stress in the vicinity of the juncture was reduced by 33 percent by the flexibility of the tapered rings. Furthermore, the nearly optimum design was assumed for the rigid ring while no attempt had been made to optimize the design of the tapered-ring juncture. Thus it appears likely that discontinuity stresses at such junctures can be appreciably reduced with tapered rings of reasonable dimensions and that an experimental invesitgation would be worthwhile to obtain some verification.

It should be pointed out that in the analysis presented herein only the discontinuity stresses arising at junctures of shell elements of different stiffnesses have been considered. Additional highly localized stresses due to notch effects at such junctures have been neglected. These latter stresses should be less severe when tapered rings are used.

ACKNOWLEDGMENTS

This work is essentially the same as that submitted by the author as a thesis to the Graduate School of the University of Maryland in July 1960 in partial fulfillment of the requirements for the degree of Master of Science. The helpful advice and criticism contributed by Prof. J.W. Jackson of the University of Maryland and Mr. J.G. Pulos of the David Taylor Model Basin are gratefully acknowledged.

REFERENCES

1. Meissner, E., "Über Elastiziatat and Festigkeit dünner Schalen," Vierteljahrsschr. Naturforsch. Ges. Zurich, Vol. 60, p. 23 (1915).

2. Horvay, G., Linkous, C., and Born, J.S., "Analysis of Short Thin Axisymmetrical Edge Loading," Journal of Applied Mechanics, Vol. 23, No. 1 (Mar 1956).

3. Timoshenko, S., "Theory of Plates and Shells," McGraw-Hill Book Company, Inc., New York (1940).

4. Hetenyi, M., "Beams on Elastic Foundation," The University of Michigan Press, Ann Arbor (1946).

5. Raetz, R.V. and Pulos, J.G., "A Procedure for Computing Stresses in a Conical Shell near Ring Stiffeners or Reinforced Intersections," David Taylor Model Basin Report 1015 (Apr 1958).

6. Frocht, M.M., "Photoelasticity," John Wiley and Sons, Inc., New York, N.Y., Vol. II (1948).

7. Taylor, C.E. and Wenk, E., Jr., "Analysis of Stress in the Conical Elements of Shell Structures," David Taylor Model Basin Report 981 (May 1956).

8. Raetz, R.V., "An Experimental Investigation of the Strength of Small-Scale Conical Reducer Sections between Cylindrical Shells under External Hydrostatic Pressure," David Taylor Model Basin Report 1397 (Mar 1960).

9. Jahnke, E. and Emde, F., "Tables of Functions," Dover Publications, New York, N.Y. (1945).

INITIAL DISTRIBUTION

Copies

14 CHBUSHIPS
- 3 Tech Info Br (Code 335)
- 1 Tech Asst (Code 106)
- 1 Lab & Programs Br (Code 321)
- 1 Prelim Des Br (Code 420)
- 1 Prelim Des Sec (Code 421)
- 1 Ship Protec (Code 423)
- 1 Hull Des Br (Code 440)
- 2 Sci & Res Sec (Code 442)
- 1 Struc Sec (Code 443)
- 1 Sub Br (Code 525)
- 1 Hull Arrgt, Struc, & Preserv (Code 633)

3 CHONR
- 2 Struc Mech Br (Code 439)
- 1 Undersea Programs (Code 466)

1 CNO (Op 702C)

1 CDR, USNOL

1 DIR, USNRL (Code 2027)

2 NAVSHIPYD PTSMH

2 NAVSHIPYD MARE

1 NAVSHIPYD NORVA, Attn: UERD (Code 280)

1 SUPSHIP, Groton

1 Electric Boat Div, General Dynamics Corp

1 SUPSHIP, Newport News

1 NNS & DD Co

1 SUPSHIP, Pascagoula

1 Ingalls Shipbldg Corp

1 Dir of Def R & E, Attn: Tech Library

1 CO, USNROTC & NAVADMINU, MIT

1 O in C, PGSCOL, Webb

10 CDR, ASTIA

1 OTS, Dept Comm

1 Mr. H. Becker, College of
Engin, New York Univ,
New York

David Taylor Model Basin. Report 1444.
ANALYSIS OF STRESSES AT JUNCTURES OF AXISYMMETRIC SHELLS WITH FLEXIBLE INSERT RINGS OF LINEARLY VARYING THICKNESS, by Richard V. Raetz. Jan 1961. v, 41p. illus., graphs, tables, refs. UNCLASSIFIED

The elastic deformations of a short, flexible, tapered ring under axisymmetric edge loading and uniform pressure are investigated. The ring is treated as a thin cylindrical or conical shell of short length and linearly varying thickness. A modified Geckeler-type approximation is used for the conical shell. Equations are derived for the elastic behavior of some typical shell junctures utilizing insert rings with tapered sections. A numerical example is given which indicates that maximum discontinuity stresses in a typical reinforced cone-cylinder juncture would be reduced by 33 percent by use of a flexible, tapered ring. The additional highly localized stresses due to notch effects have not been considered.

1. Conical shells--Stresses--Mathematical analysis
2. Conical shells--Deformation--Mathematical analysis
I. Raetz, Richard V.
II. S-F013 03 02

David Taylor Model Basin. Report 1444.
ANALYSIS OF STRESSES AT JUNCTURES OF AXISYMMETRIC SHELLS WITH FLEXIBLE INSERT RINGS OF LINEARLY VARYING THICKNESS, by Richard V. Raetz. Jan 1961. v, 41p. illus., graphs, tables, refs. UNCLASSIFIED

The elastic deformations of a short, flexible, tapered ring under axisymmetric edge loading and uniform pressure are investigated. The ring is treated as a thin cylindrical or conical shell of short length and linearly varying thickness. A modified Geckeler-type approximation is used for the conical shell. Equations are derived for the elastic behavior of some typical shell junctures utilizing insert rings with tapered sections. A numerical example is given which indicates that maximum discontinuity stresses in a typical reinforced cone-cylinder juncture would be reduced by 33 percent by use of a flexible, tapered ring. The additional highly localized stresses due to notch effects have not been considered.

1. Conical shells--Stresses--Mathematical analysis
2. Conical shells--Deformation--Mathematical analysis
I. Raetz, Richard V.
II. S-F013 03 02